6

Magnetic domains

Magnetization reversal in thin films and some relevant experimental methods

Maciej Urbaniak

IFM PAN 2012

Today's plan

- Magnetic domains
- Domain walls
- Single domain particles, superparamagnetism
- Magnetic domains in bulk systems
- Magnetic domains in thin films

Magnetic domains – early views

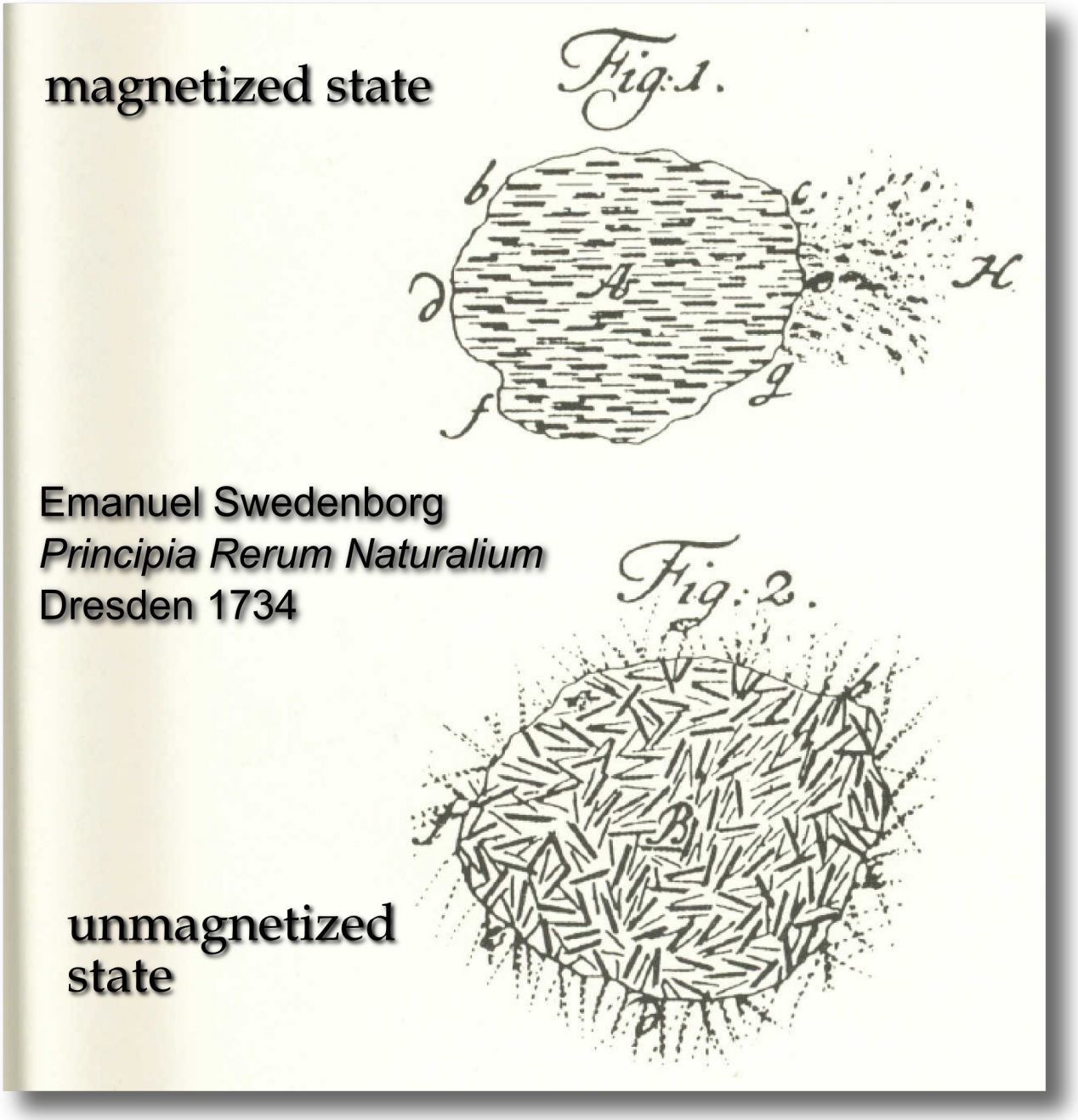

original image taken from:
B. D. Cullity
Introduction to magnetic materials
Addison-Wesley, Reading,
Massachusetts 1972

Magnetic domains - preliminaries

•Real ferromagnets at zero applied field are usually divided into domains which are magnetized in different directions [1,2,3]

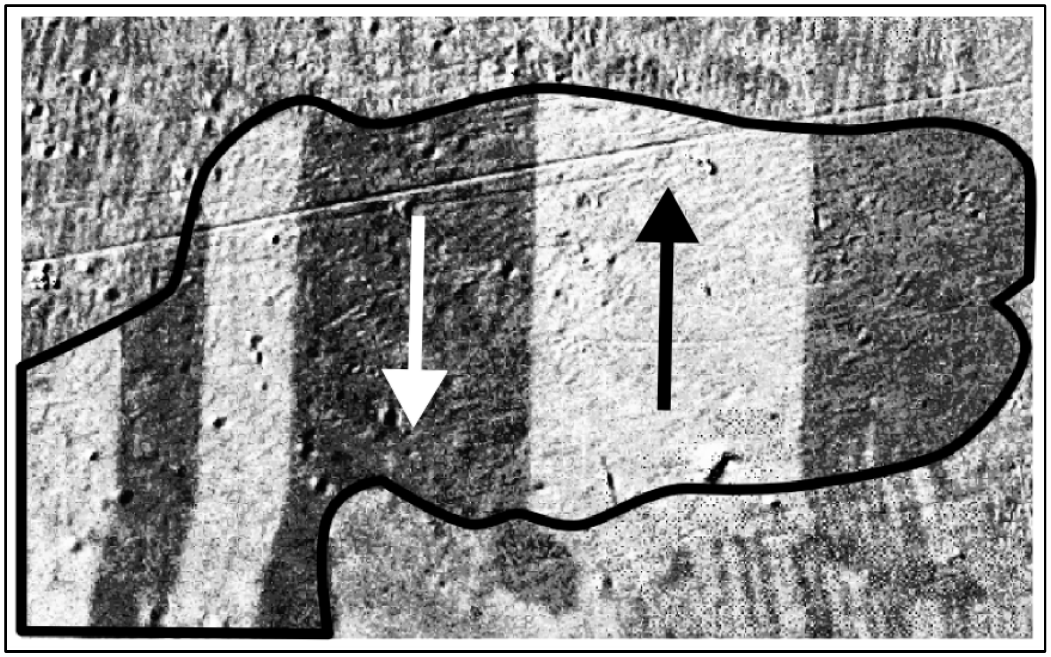

Magnetic domains in a **single grain** (outlined with a black line) of **non-oriented electrical steel**. The photo shows an area 0.1 mm wide. The sample was polished and photographed under **Kerr-effect microscope**. The polishing was not perfect - there is an angled scratch through the whole width of image (top half of the photo). The area outside of the grain has different crystallographic orientation, so the domain structure is much more complex. The arrows show the direction of magnetisation in each domain - all white domains are magnetised "up", all dark domains are magnetised "down".

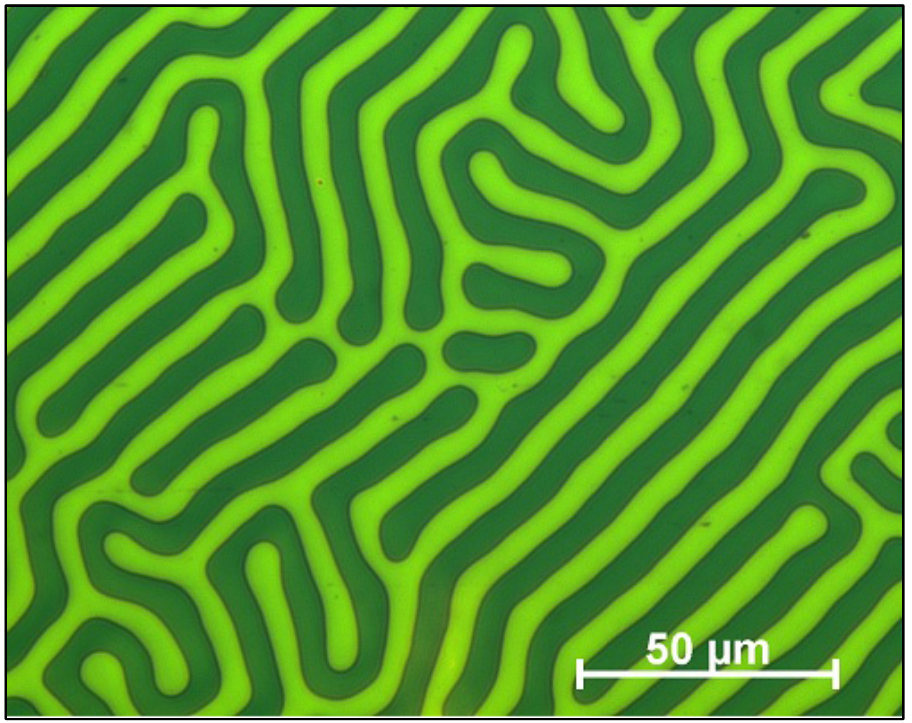

Visualization of meandering domains (image taken with CMOS-MagView).

Typically the magnetic domains are of 10-100µm size

Magnetic domains - preliminaries

- Real ferromagnets at zero applied field are divided into domains which are magnetized in different directions [1,2,3]
- Barkhausen noise was the first confirmation of the domain concept [3].

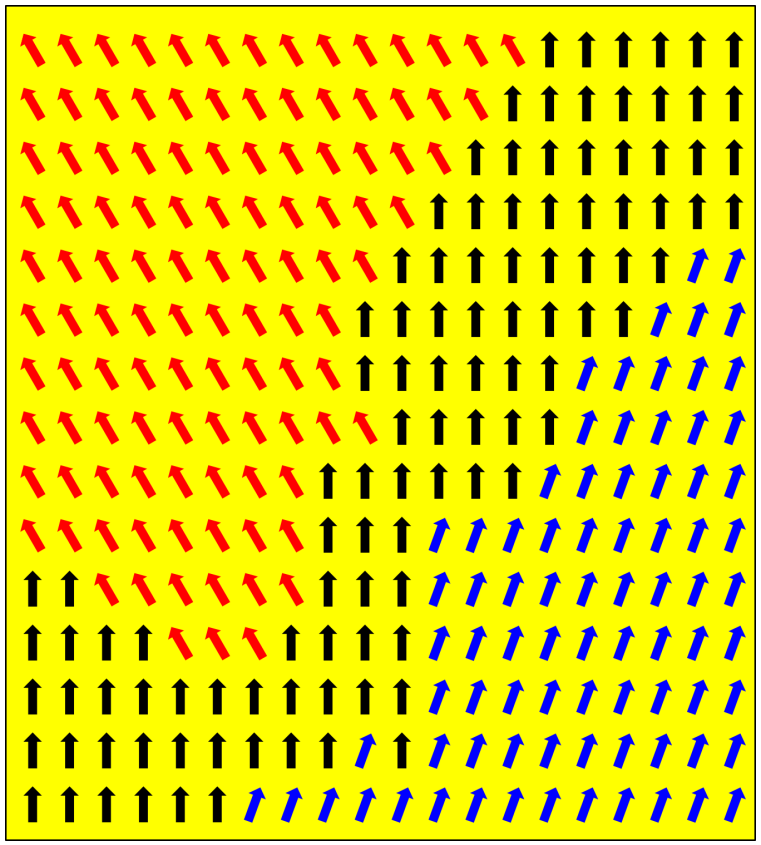

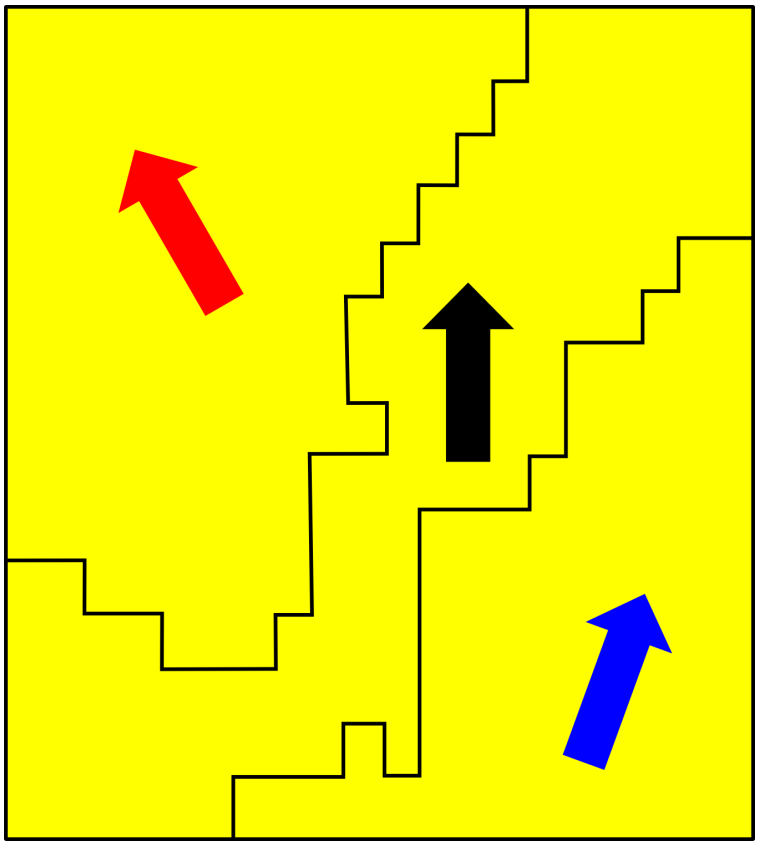

- Usually it can be safely assumed that magnetic moment direction within a given domain is constant in areas distant from the boundaries with other domains (domain walls)

Magnetic domains - preliminaries

•Magnetic domains are of magnetostatic origin and their shapes and sizes can be calculated within the classical electrodynamics*:

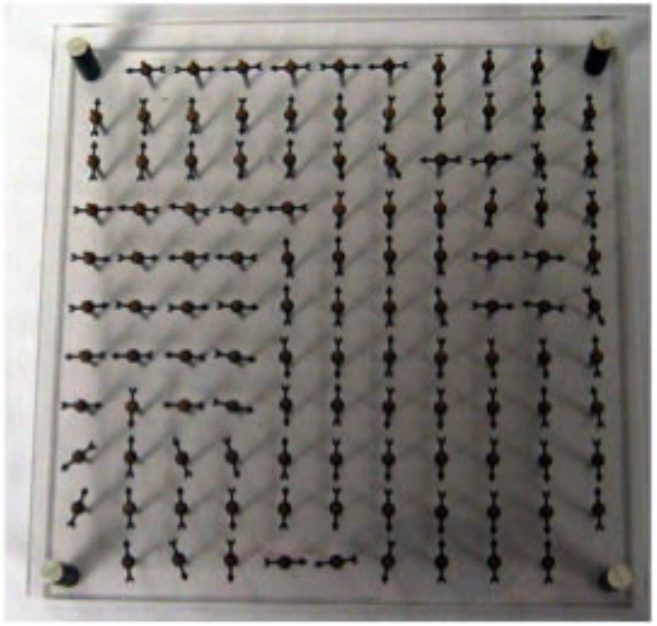

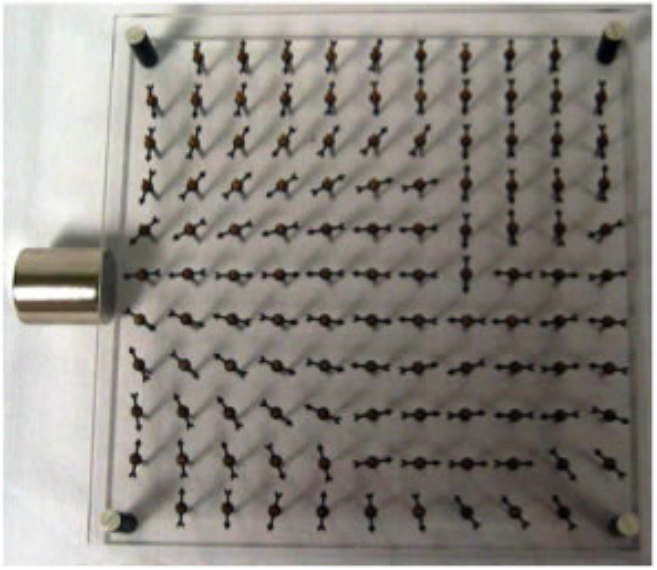

images source: http://www.ece.neu.edu/faculty/nian/mom/domains.html

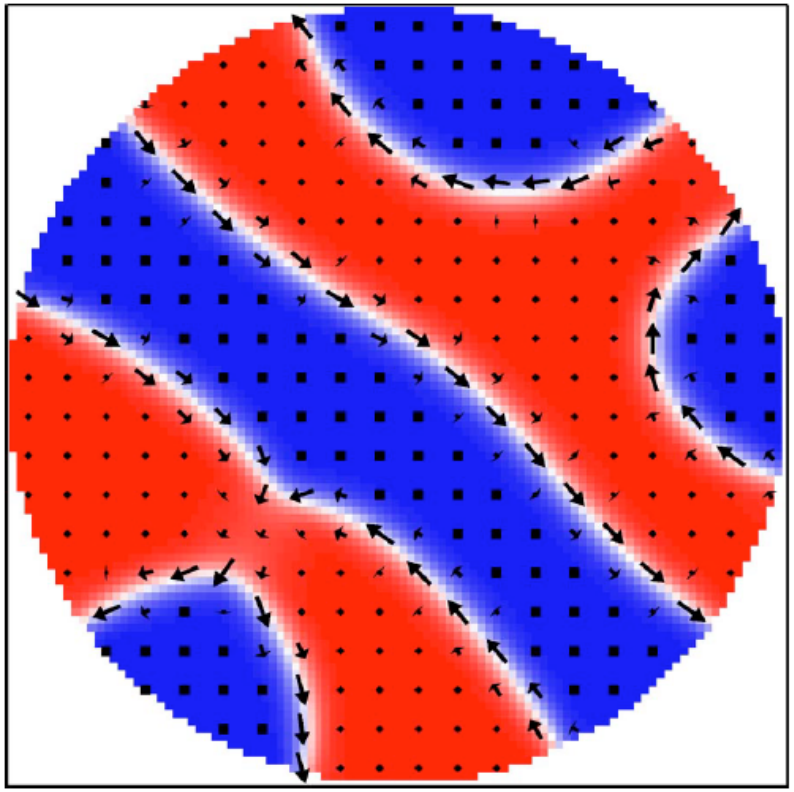

D. Clarke, O. A. Tretiakov, and O. Tchernyshyov, PHYSICAL REVIEW B **75**, 174433 (2007)

FIG. 5. (Color online) A stationary configuration obtained from a random initial state in a disk of thickness of 14 nm and diameter of 400 nm. Magnetization length $M=1.4\times10^6$ A/m, exchange constant $A=3.3\times10^{-11}$ J/m, exchange length $\lambda=5.2$ nm, and easy-axis anisotropy $K=1.5\times10^6$ J/m^3 yield $\kappa=0.22$ and $\kappa_0=0.45$. Magnetization points up in the red (light gray) regions and down in the blue (dark gray) regions. Numerical simulation using OOMMF (Ref. 18).

*quantum mechanics enters through exchange, anisotropy etc. constants

Magnetic domains - preliminaries

- Magnetic domains visualized in bulk materials (propagation of volume magnetization)
- Neutron refraction at domain walls allows the visualization of the domain structure.

C. Grünzweig, C. David, O. Bunk, J. Kohlbrecher, E. Lehmann et al., J. Appl. Phys. 107, 09D308 (2010)

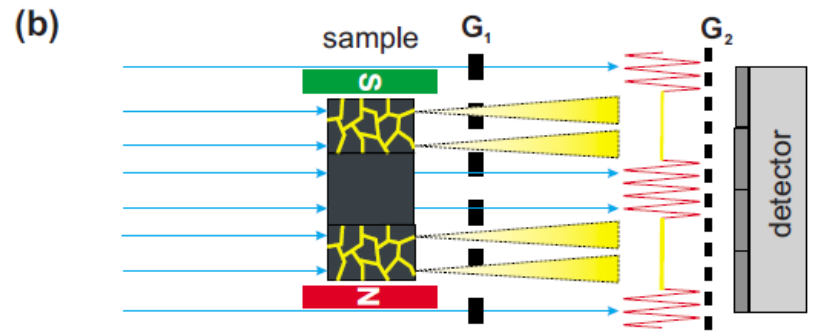

FIG. 1. (Color online) (a) Setup with the source grating G_0, the phase grating G_1, the analyzer absorption grating G_2, and an electromagnet creating a horizontal variable magnetic field around the sample. (b) Multiple refraction of neutrons at magnetic domain walls in the sample causes a local degradation of the coherence of the neutron wave field and results in a decrease of the local fringe visibility of the interference pattern.

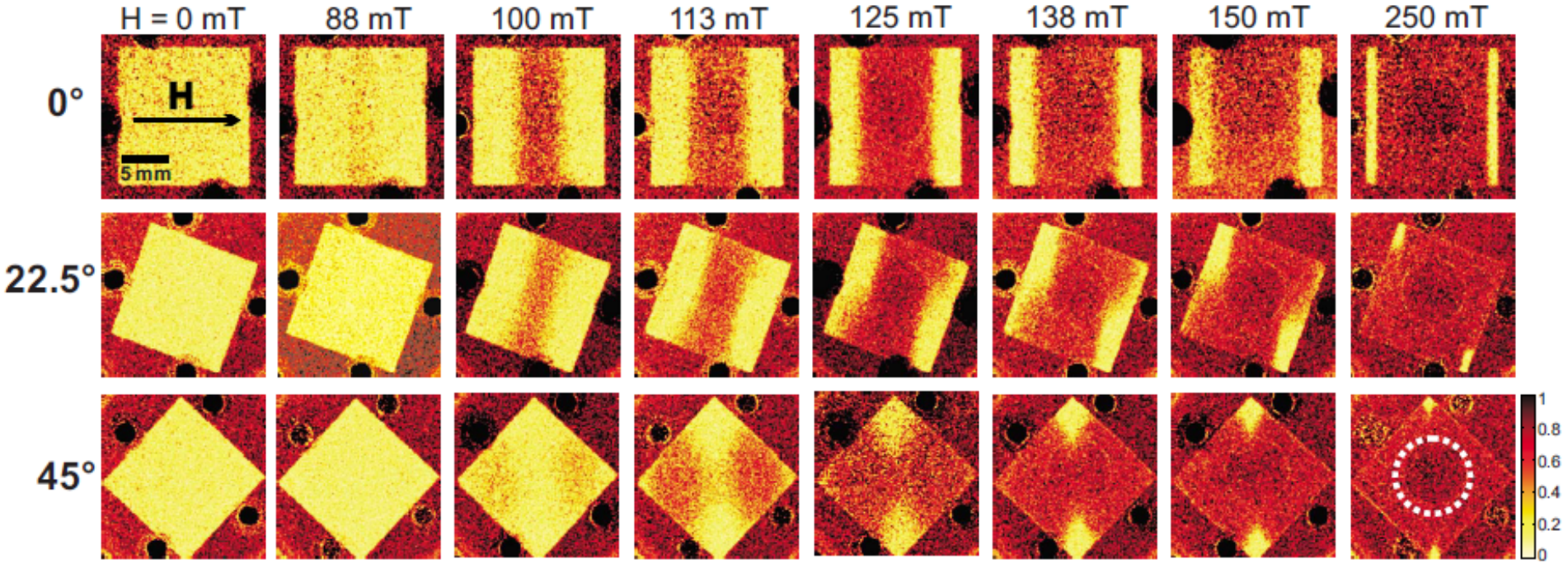

FIG. 2. (Color online) Neutron DFIs of the geometry-dependent magnetization process of the polycrystalline steel plate for different orientations ω=0°, 22.5°, and 45°. Different magnetization behaviors and starting points of the propagation of the volume magnetization for each orientation are observed. The yellow color in the DFIs indicates domain wall-rich areas.

Origin of magnetic domains

•Consider a infinite cylinder, with 2R diameter, magnetized uniformly:

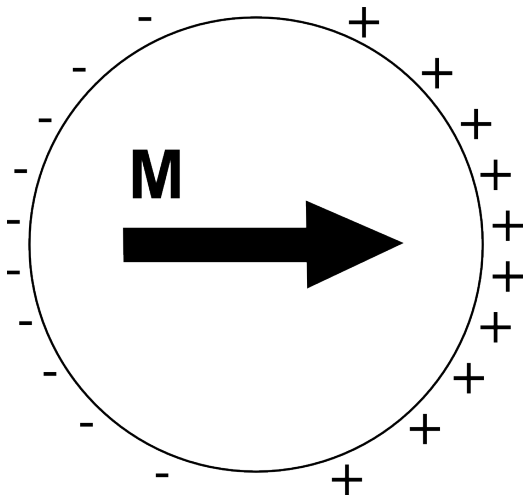

$$\rho_{magn} = -\nabla \cdot \vec{M}$$

•The discontinuity of magnetization at outer boundaries creates magnetic charges at the surface of the cylinder (see L.2)

$$\phi_m(\vec{r}) = \oint_S \frac{\vec{M}\cdot\vec{ds}}{|\vec{r}|} - \int_V \frac{\nabla\cdot\vec{M}}{|\vec{r}|} d^3 r'$$

•Using the expression for the shape anisotropy energy (from L.5): we obtain for the energy per unit length along z:

$$E_{demag} = \frac{1}{2} V \mu_0 (N\cdot\vec{M})\cdot\vec{M},$$

$$V - volume \quad of \quad the \quad sample$$

$$E_{demag} = \frac{1}{2}\mu_0 \frac{1}{2} M_S^2 \pi R^2 = \mu_0 \frac{\pi}{4} R^2 M_S^2$$

demag factor for cylinder $N_x + N_y + N_z = 1$

Origin of magnetic domains

•Consider now a infinite cylinder magnetized as shown below (i.e., divided into two antiparallel domains):

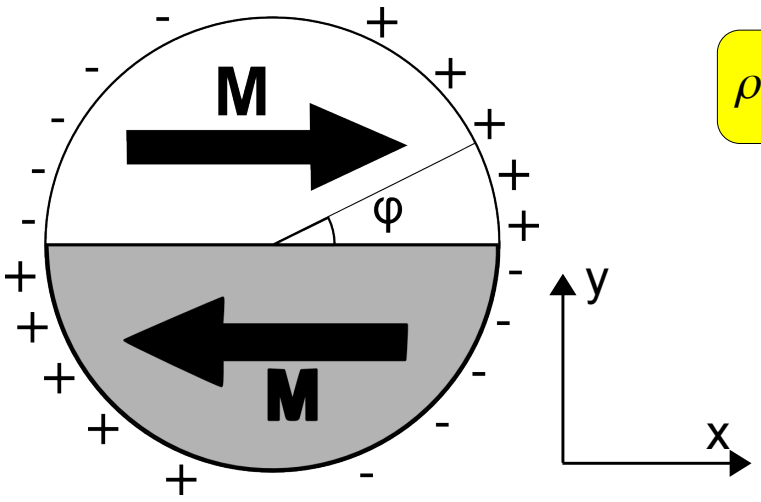

$$\rho_{magn} = -\nabla \cdot \vec{M}$$

•It is assumed that both domains are of equal sizes
•The division into the domains changes the distribution of magnetic surface charges over the surface of the cylinder

•We outline now the derivation of the demagnetization energy of the two-domain cylinder (that part is taken from A. Aharoni [2]).
•The magnetization is:

$$M_y = M_z = 0, \qquad M_x = M_s \times \begin{pmatrix} +1 & if & y > 0, & i.e., & 0 \le \varphi \le \pi \\ -1 & if & y,0, & i.e., & \pi \le \varphi \le 2\pi \end{pmatrix}$$

Origin of magnetic domains

- The step function can be expressed as a Fourier expansion:

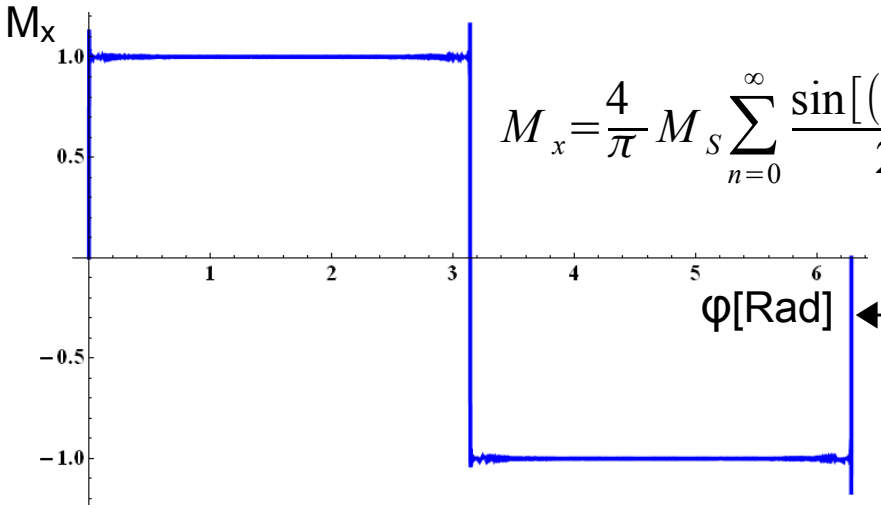

$$M_x = \frac{4}{\pi} M_S \sum_{n=0}^{\infty} \frac{\sin[(2n+1)\phi]}{2n+1}$$

for n_{max}=1000

$$\cos\alpha \sin\beta = \frac{1}{2}\left(\sin(\alpha+\beta)+\sin(\alpha-\beta)\right)$$

- The normal component of magnetization (i.e., the one creating magnetic charges) is then:

$$M_n = M_\rho = M_x \cos(\phi) = \frac{2}{\pi} M_S \sum_{n=0}^{\infty} \frac{\sin[(2n+2)\phi]+\sin[2n\phi]}{2n+1}$$

1 $\sin[(2n+2)\phi] = \sin[(2n+1)\phi+\phi] = 2\sin[(2n+1)\phi]\cos(\phi) - \sin(2n\phi)$

$$\sin[(2n+1)\phi]\cos(\phi) = \frac{1}{2}[\sin[(2n+2)\phi]+\sin(2n\phi)]$$

- The sum can be broken down into two sums [2]:

$$M_n = \frac{2}{\pi} M_S \sum_{n=1}^{\infty} \left[\frac{1}{2n-1} + \frac{1}{2n+1}\right] \sin[2n\phi]$$

the second term is null for n=0 and in the first term
n is replaced by (n-1) so that the sum starts effectively from n=0

$$n \to n-1: \quad \frac{\sin[(2n+2)\phi]}{2n+1} \to \frac{\sin(2n\phi)}{2n-1}$$

Origin of magnetic domains

•The boundary condition, at cylinder surface, for magnetic scalar potential *U* is [2]:

$$\left(\frac{\partial}{\partial \rho}U_{inside}-\frac{\partial}{\partial \rho}U_{outside}\right)_{\rho=Radius}=M_n=\frac{8}{\pi}M_S\sum_{n=1}^{\infty}\frac{n\sin(2n\phi)}{(2n+1)(2n-1)}$$

$$\frac{1}{2n-1}+\frac{1}{2n+1}=\frac{4n}{(2n+1)(2n-1)}$$

•We seek a solution of the form (guessing):

$$U=\sum_{n=1}^{\infty}u_n(\rho)\sin(2n\phi)$$

•Since magnetization is constant throughout the domains we have $\nabla^2 U=0$ and:

$$\nabla^2 U=\sum_{n=1}^{\infty}\sin(2n\phi)\left(\frac{\partial^2}{\partial\rho^2}+\frac{1}{\rho}\frac{\partial}{\partial\rho}-\frac{4n^2}{\rho^2}\right)u_n(\rho)$$

Laplacian in cylindrical coordinates:

$$\nabla^2 f=\frac{1}{r}\frac{\partial}{\partial r}\left(r\frac{\partial}{\partial r}f\right)+\frac{1}{r^2}\frac{\partial^2}{\partial\phi^2}f+\frac{\partial^2}{\partial z^2}f$$

•Because we are calculating demagnetization energy we need only magnetic field within the cylinder. The solutions to *differential equation* in the Laplacian of *U* are*:

$$u_n(\rho)=c_n\times\begin{pmatrix}(\rho/R)^{2n} & if\ \rho\le R\\ (\rho/R)^{-2n} & if\ \rho\ge R\end{pmatrix}$$

*negative powers are introduced to have vanishing potential at infinity; constant R is introduced to comply with magnetostatic problem - ρ^n is a solution too.

Origin of magnetic domains

•The boundary condition, at cylinder surface, for magnetic scalar potential *U* is [2]:

$$\left(\frac{\partial}{\partial \rho}U_{inside}-\frac{\partial}{\partial \rho}U_{outside}\right)_{\rho=Radius}=M_n=\frac{8}{\pi}M_S\sum_{n=0}^{\infty}\frac{n\sin(2n\phi)}{(2n+1)(2n-1)}$$

$$\frac{1}{2n-1}+\frac{1}{2n+1}=\frac{4n}{(2n+1)(2n-1)}$$

•We seek a solution of the form (guessing):

$$U=\sum_{n=1}^{\infty}u_n(\rho)\sin(2n\phi)$$

•Since magnetization is constant throughout the domains we have $\nabla^2 U=0$ and:

$$\nabla^2 U=\sum_{n=1}^{\infty}\sin(2n\phi)\left(\frac{\partial^2}{\partial\rho^2}+\frac{1}{\rho}\frac{\partial}{\partial\rho}-\frac{4n^2}{\rho^2}\right)u_n(\rho)$$

Laplacian in cylindrical coordinates:

$$\nabla^2 f=\frac{1}{r}\frac{\partial}{\partial r}\left(r\frac{\partial}{\partial r}f\right)+\frac{1}{r^2}\frac{\partial^2}{\partial\phi^2}f+\frac{\partial^2}{\partial z^2}f$$

•Because we are calculating demagnetization energy we need only magnetic field within the cylinder. The solutions to *differential equation* in the Laplacian of *U* are*:

$$u_n(\rho)=c_n\times\begin{pmatrix}(\rho/R)^{2n} & if\ \rho\le R\\ (\rho/R)^{-2n} & if\ \rho\ge R\end{pmatrix}$$

*negative powers are introduced to have vanishing potential at infinity; constant R is introduced to comply with magnetostatic problem - ρ^n is a solution too.

Origin of magnetic domains

•After substitution of U_{inside} and $U_{outside}$ we have:

$$\sum_{n=1}^{n} c_n\left(\frac{2n}{R}+\frac{2n}{R}\right)\sin(2n\phi)=\frac{8}{\pi}M_S\sum_{n=1}^{\infty}\frac{n\sin(2n\phi)}{(2n+1)(2n-1)} \quad \Rightarrow \quad c_n=\frac{2M_S R}{\pi(2n+1)(2n-1)}$$

•And the potential inside the cylinder is:

$$U_{inside}=\frac{2}{\pi}RM_S\sum_{n=1}^{\infty}\frac{\sin(2n\phi)}{(2n+1)(2n-1)}\left(\frac{\rho}{R}\right)^{2n} \longleftarrow U=\sum_{n=1}^{\infty}u_n(\rho)\sin(2n\phi)$$

•The field inside the cylinder is obtained from gradient of U [2]:

$$H_x^{inside}=-\frac{\partial}{\partial x}U_{inside}=-\left(\cos\phi\frac{\partial}{\partial\rho}-\frac{\sin\phi}{\rho}\frac{\partial}{\partial\phi}\right)U_{inside}$$

We need only H_x since:

$$M_y=M_z=0$$

•The demagnetizing energy is given by:

$$E_{demag}=-\frac{1}{2}\int_{\rho\le R}\vec{M}\cdot\vec{B}\,dV=-\frac{1}{2}\mu_0\int_{\rho\le R}M_x H_x^{inside}\,dV$$

•We leave out the integration [see 2] and have for the demagnetizing energy per unit length of the cylinder:

$$E_{demag}=\frac{1}{\pi}\mu_0 R^2 M_s^2$$

Origin of magnetic domains

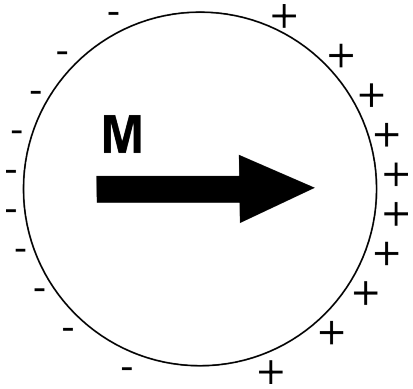

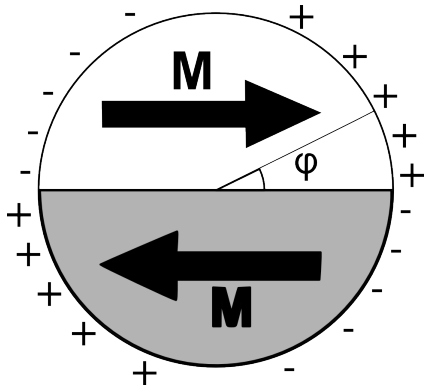

$$E_{demag}^{one\ domain} = \mu_0 \frac{\pi}{4} R^2 M_S^2$$

$$E_{demag}^{two\ domains} = \mu_0 \frac{1}{\pi} R^2 M_s^2$$

•The demagnetization energy of the cylinder with one domain is higher that that with two domains:

$$\frac{E_{demag}^{one\ domain}}{E_{demag}^{two\ domains}} = \frac{\pi^2}{4} > 1 \quad \approx 2.5$$

•The result does not depend on the radius or the saturation magnetization of cylinder.

•It may be surmised that for any ferromagnetic material the magnetostatic energy may be reduced by subdividing the crystal into at least two domains.

Magnetostatic interactions favor the subdivision of the crystal into magnetic domains

Potential energy of magnetic charge - digression

In many cases instead of calculating energy of a magnetic body in the external field from the formula:

$$E_{magn} = -\int \vec{M}\cdot\vec{B}\,dV = -\int \vec{J}\cdot\vec{H}\,dV$$

one can use *magnetic charge* method and the *magnetic scalar potential* (lecture 2): $\vec{H} = -\nabla\phi$

$$E_{magn} = -\mu_0\int \vec{M}\cdot\vec{H}\,dV = \mu_0\int \vec{M}\cdot\nabla\phi\,dV = \mu_0\int (\hat{x}M_x + \hat{y}M_y + \hat{z}M_z)\cdot(\hat{x}\frac{\partial}{\partial x}\phi + \hat{y}\frac{\partial}{\partial y}\phi + \hat{z}\frac{\partial}{\partial z}\phi)\,dV =$$

$$\mu_0\int (M_x\frac{\partial}{\partial x}\phi + M_y\frac{\partial}{\partial y}\phi + M_z\frac{\partial}{\partial z}\phi)\,dV =$$

$$\mu_0\int [(\frac{\partial}{\partial x}M_x\phi - \phi\frac{\partial}{\partial x}M_x) + (\frac{\partial}{\partial y}M_y\phi - \phi\frac{\partial}{\partial y}M_y) + (\frac{\partial}{\partial z}M_z\phi - \phi\frac{\partial}{\partial z}M_z)]\,dV =$$

$$\mu_0\int (\frac{\partial}{\partial x}M_x\phi + \frac{\partial}{\partial y}M_y\phi + \frac{\partial}{\partial z}M_z\phi)\,dV - \mu_0\int (\phi\frac{\partial}{\partial x}M_x + \phi\frac{\partial}{\partial y}M_y + \phi\frac{\partial}{\partial z}M_z)\,dV =$$

$$\mu_0\int \nabla\cdot(\phi\vec{M})\,dV - \mu_0\int \phi\,\nabla\cdot\vec{M}\,dV = \mu_0\int_{surface} \phi\,\vec{M}\,dS + \mu_0\int \phi\,\rho_{magn}\,dV$$

from Gauss divergence theorem

Magnetic charge (L.2):

$$\rho_{magn} = -\nabla\cdot\vec{M}$$

$$E_{magn} = \mu_0\int_{surface} \phi\,\vec{M}\,dS + \mu_0\int \phi\,\rho_{magn}\,dV$$

A. Hubert, W. Rave, S.L. Tomlinson, phys. stat. sol. (b) 204, 817 (1997)

Potential energy of magnetic charge - digression

In many cases instead of calculating energy of a magnetic body in the external field from the formula:

$$E_{magn} = -\int \vec{M} \cdot \vec{B}\, dV = -\int \vec{J} \cdot \vec{H}\, dV$$

one can use *magnetic charge* method and the *magnetic scalar potential* (lecture 2): $\vec{H} = -\nabla \phi$

If body is magnetized uniformly (no volume magnetic charges) to obtain its magnetostatic energy in external field it is enough to evaluate surface integral of surface charges times the scalar magnetic potential on the surface:

$$E_{magn} = \mu_0 \int_{surface} \phi\, \vec{M}\, dS$$

$\vec{M} \cdot \vec{dS}$ - surface magnetic charge

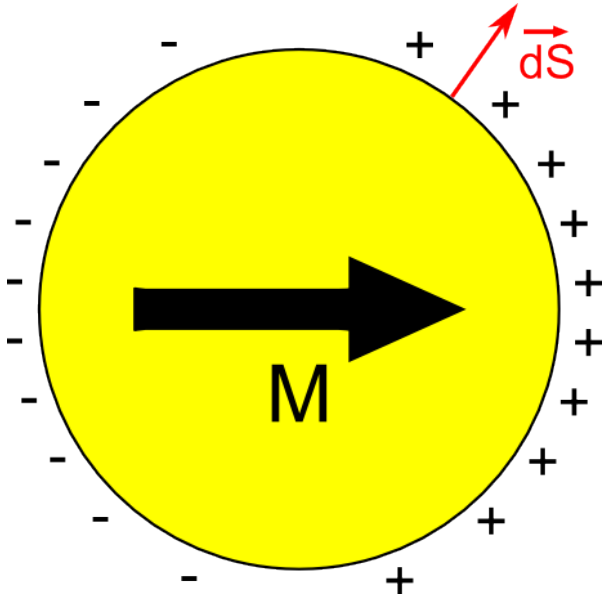

$$E_{magn} = \mu_0 \int_{surface} \phi\, \vec{M}\, dS + \mu_0 \int \phi\, \rho_{magn}\, dV$$

A. Hubert, W. Rave, S.L. Tomlinson, phys. stat. sol. (b) 204, 817 (1997)

Origin of magnetic domains

- The calculations performed for other geometries* lead to the same conclusions.
- It can be shown that further subdivision can reduce further the magnetostatic self energy [2].

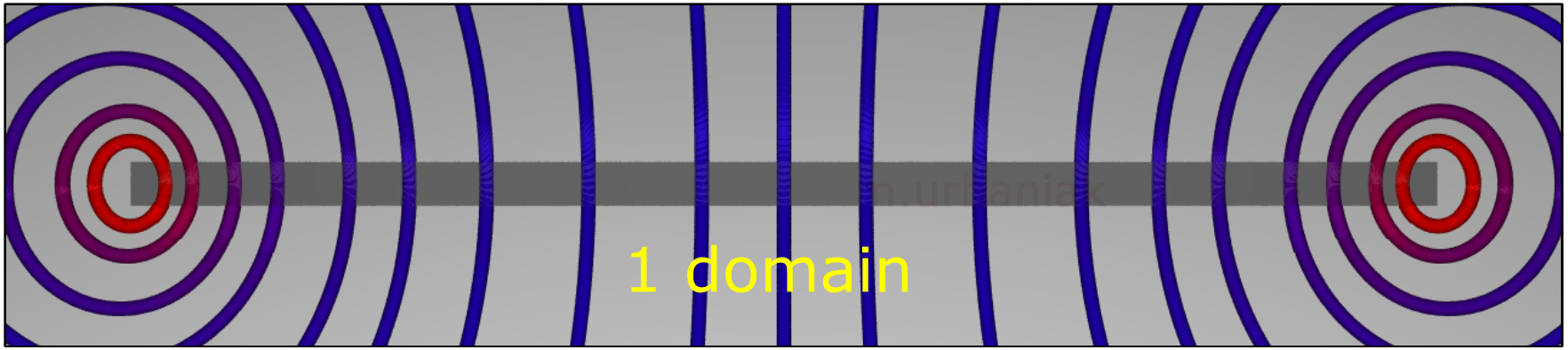

The division into domains increases magnetic induction ***B*** within the magnetic film and decreases magnetostatic energy – **stripe domain structure appears**.

$$E_{magn} = -\vec{B} \cdot \vec{M}$$

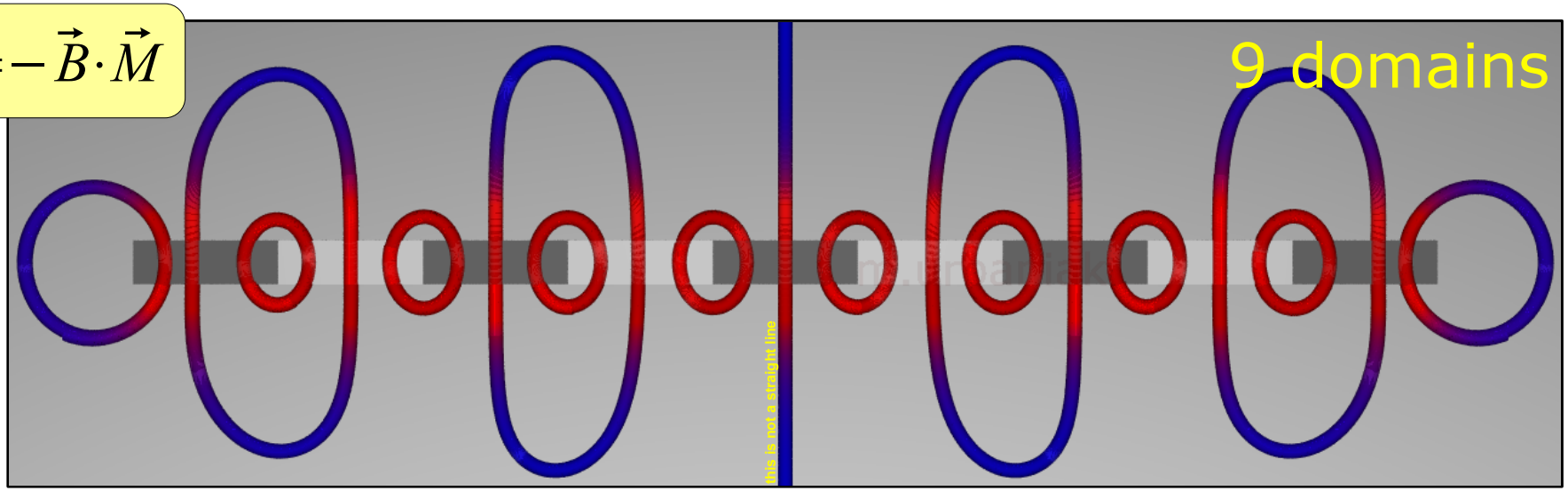

* A. Aharoni obtained the similar expressions for a sphere J. Appl. Phys. **51**, 5906 (1980)

Domain walls

•The exchange energy of a pair of spins, making an angle φ, located on neighboring atoms can be expressed as [1]:

$$E_{ex} = -2 J S^2 \cos\phi_{ij} \qquad \cos\phi = 1 - \phi^2/2 + \phi^4/24 - \ldots$$

•For small angles the variable part of energy can be written as:

$$E_{ex} = J S^2 \phi_{ij}^2$$ The lower the interspin angle the lower the exchange energy

•Consider a line of uniformly spaced spins (atoms) gradually changing uniformly their orientation from down to up through N atomic layers.
For that case we have:

$$\phi_{ij} = \pi / N$$

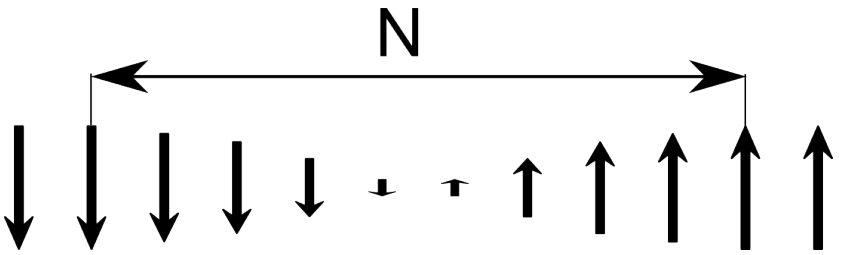

•For a simple cubic structure with lattice spacing *a* there is $1/a^2$ spin pairs per unit area of (100) surfaces.
The exchange energy stored per square meter is then:

$$E_{ex} = N\left(\frac{1}{a^2}\right)^2 \times J S^2 \left(\frac{\pi}{N}\right)^2 = \frac{J S^2 \pi^2}{a^2 N} \propto \frac{1}{N}$$

The larger the width of transition region in 180° wall the lower the exchange energy stored in transition region

Domain walls

- The deviation of spin directions within the transition region from easy directions of magnetocrystalline anisotropy results in a increase of anisotropy energy.
- That increase in energy, per unit area, can be approximated, *very roughly* by [1]:

$$E_A = K \times thickness \quad of \quad transition \quad region = K \times N\, a$$

- The total (magnetocrystalline and exchange) energy of transition region is thus:

$$E_{total} = E_{ex} + E_A = \frac{J\, S^2\, \pi^2}{a^2\, N} + KNa$$

- The energy is minimum with respect to N for:

$$N = \sqrt{\frac{J\, S^2\, \pi^2}{K\, a^3}}$$

- And the corresponding transition region thickness, i.e., the thickness of domain wall is:

$$\delta = Na = \sqrt{\frac{J\, S^2\, \pi^2}{K\, a}} \qquad \Rightarrow \qquad \delta \propto \sqrt{\frac{J}{K}}$$

- For iron the above expressions predict domain wall thickness of approx. 42 nm which corresponds roughly to 150 lattice constants *a* [1].

Domain walls

- The preliminary assumption of the uniform rotation of spins within the domain wall must be determined/confirmed from the equilibrium condition [1].
- We assume that at $z=-\infty$ the spin angle is $-\pi/2$ and at $z=+\infty$ the spin angle is $\pi/2$.
- In continuum approximation the angle between the neighboring spins is given by [1]:

$$\Delta\phi = \left(\frac{\partial\phi}{\partial z}\right) a$$

- And the exchange energy per spin pair is:

$$E_{ex} = J S^2 a^2 \left(\frac{\partial\phi}{\partial z}\right)^2 \qquad E_{ex} = J S^2 \phi_{i\,j}^2$$

- The exchange energy per unit area of the wall can be thus expressed as:

$$\gamma_{ex} = \frac{1}{a^2} J S^2 a^2 \int_{-\infty}^{+\infty} \left(\frac{\partial\phi}{\partial z}\right)^2 \frac{1}{a} dz = \frac{J S^2}{a} \int_{-\infty}^{+\infty} \left(\frac{\partial\phi}{\partial z}\right)^2 dz$$

number of spins per unit length

number of spins per unit area of the wall

- Similarly the magntocrystalline energy (with one anisotropy constant) is given by:

$$\gamma_A = \int_{-\infty}^{+\infty} K \cos^2\phi \, dz$$

Domain walls

•The sum of the magnetocrystalline and exchange energy is then [1,3]:

$$\gamma = \gamma_{ex} + \gamma_A = \int_{-\infty}^{+\infty} \left[\frac{J S^2}{a} \left(\frac{\partial \phi}{\partial z} \right)^2 + K \cos^2 \phi \right] dz$$

•The expression $J S^2 / a$ is called a exchange stiffness constant and is usually denoted by *A*. For ferro-magnetic metals *A* is of the order of 10^{-11} J/m.

•The φ(x) function that minimizes the energy can be found with variational calculus [3]. The **Euler-Lagrange** differential equation that minimizes the integral of the form*:

$$\int f\left(x, y, \frac{dy}{dx}\right) dx \qquad \text{is} \qquad \frac{\partial f}{\partial y} - \frac{d}{dx}\left(\frac{\partial f}{\partial y_x} \right) = 0$$

$$y_x \equiv \frac{dy}{dx}$$

•Substituting the integrand of the above energy integral into *E-L* equation we get:

$$2A\left(\frac{\partial^2 \phi}{\partial z^2} \right) - 2K \sin\phi \cos\phi = 0$$

$$\cos(2\alpha) = 2\cos^2\alpha - 1$$

•Multiplying left/both sides by φ' and integrating transforms it to [3]:

$$\frac{\partial}{\partial z}\left(A\left(\frac{\partial \phi}{\partial z} \right)^2 \right) = 2A \frac{\partial \phi}{\partial z} \frac{\partial^2 \phi}{\partial z^2}$$

$$\int \left(2A\left(\frac{\partial^2 \phi}{\partial z^2} \right) - 2K \sin\phi \cos\phi \right) \frac{d\phi}{dz} dz = -\frac{1}{2} K \cos(2\phi) + A\left(\frac{\partial \phi}{\partial z} \right)^2 + C = -K\cos^2\phi + A\left(\frac{\partial \phi}{\partial z} \right)^2 + (C-1) = 0$$

*Weisstein, Eric W. "Euler-Lagrange Differential Equation." From MathWorld--A Wolfram Web Resource. http://mathworld.wolfram.com/Euler-LagrangeDifferentialEquation.html

Domain walls

•For an isolated domain wall in an infinite medium the derivative φ' at infinity must vanish [3]. We have then, with $\varphi_\infty=\pi/2$:

$$-K\cos^2\left(\frac{\pi}{2}\right)+A\left(\frac{\partial\phi}{\partial z}\right)^2+C'=0 \quad\Rightarrow\quad C'=0 \quad\Rightarrow\quad \boxed{K\cos^2\phi=A\left(\frac{\partial\phi}{\partial z}\right)^2}\ ^{*} \quad\Rightarrow\quad dz=\pm\sqrt{A/K}\,d\phi/\cos\phi$$

•Substituting this into the expression for the total energy we get:

$$\gamma=2\int_{-\infty}^{+\infty}K\cos^2\phi\,dz=2\int_{-\pi/2}^{+\pi/2}K\cos\phi\sqrt{A/K}\,d\phi=4\sqrt{AK}$$

•The energy of the 180° Bloch wall is thus: $\boxed{\gamma=4\sqrt{AK}}$

•The dependence of spin deflection as a function of *z* is obtained from the *dz* expression:

$$z=\sqrt{A/K}\int_{-\pi/2}^{+\pi/2}\frac{1}{\cos\phi}\,d\phi=2\sqrt{A/K}\tanh^{-1}\left(\tan\left(\phi/2\right)\right)$$

* at every point within the wall anisotropy energy density equals exchange energy density

Domain walls

•The z-dependence of the deflection angle of spins:

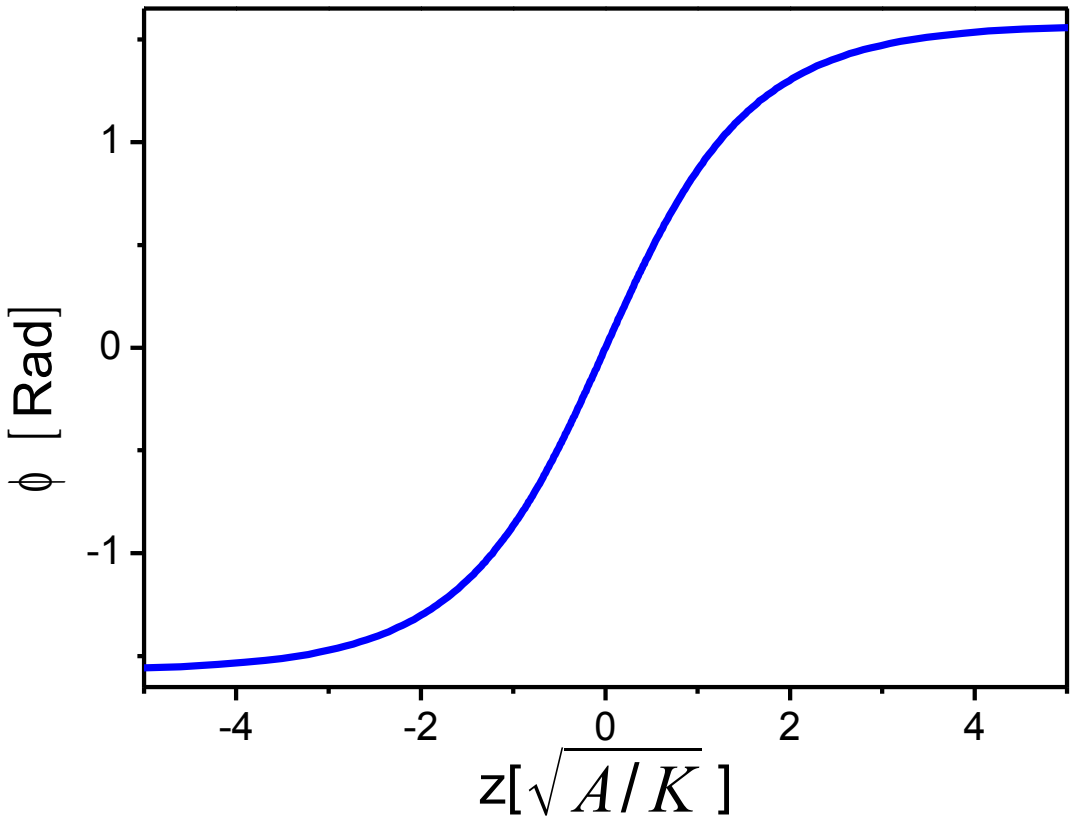

•For high values of *z* (far from the center of the domain wall the angle asymptotically approaches $\pm\pi/2$

•The Bloch wall has an infinite extent but for $z \geq 5\sqrt{A/K}$ it can be assumed to be practically saturated [3]

•That is the reason why the solution obtained for the infinite medium can be used in many practical applications

•To note is that the divergence of magnetization in **Bloch** domain wall is zero – it **does not create magnetic charges within the crystal**

$$\nabla \cdot \vec{M} = \frac{\partial M_x}{\partial x} + \frac{\partial M_y}{\partial y} + \frac{\partial M_z}{\partial z} = 0$$

•The charges exist on outer boundaries of the crystal and become important in the analysis of thin magnetic films or small magnetic particles.

Domain walls - width

•There are several definitions of the domain wall width [3].

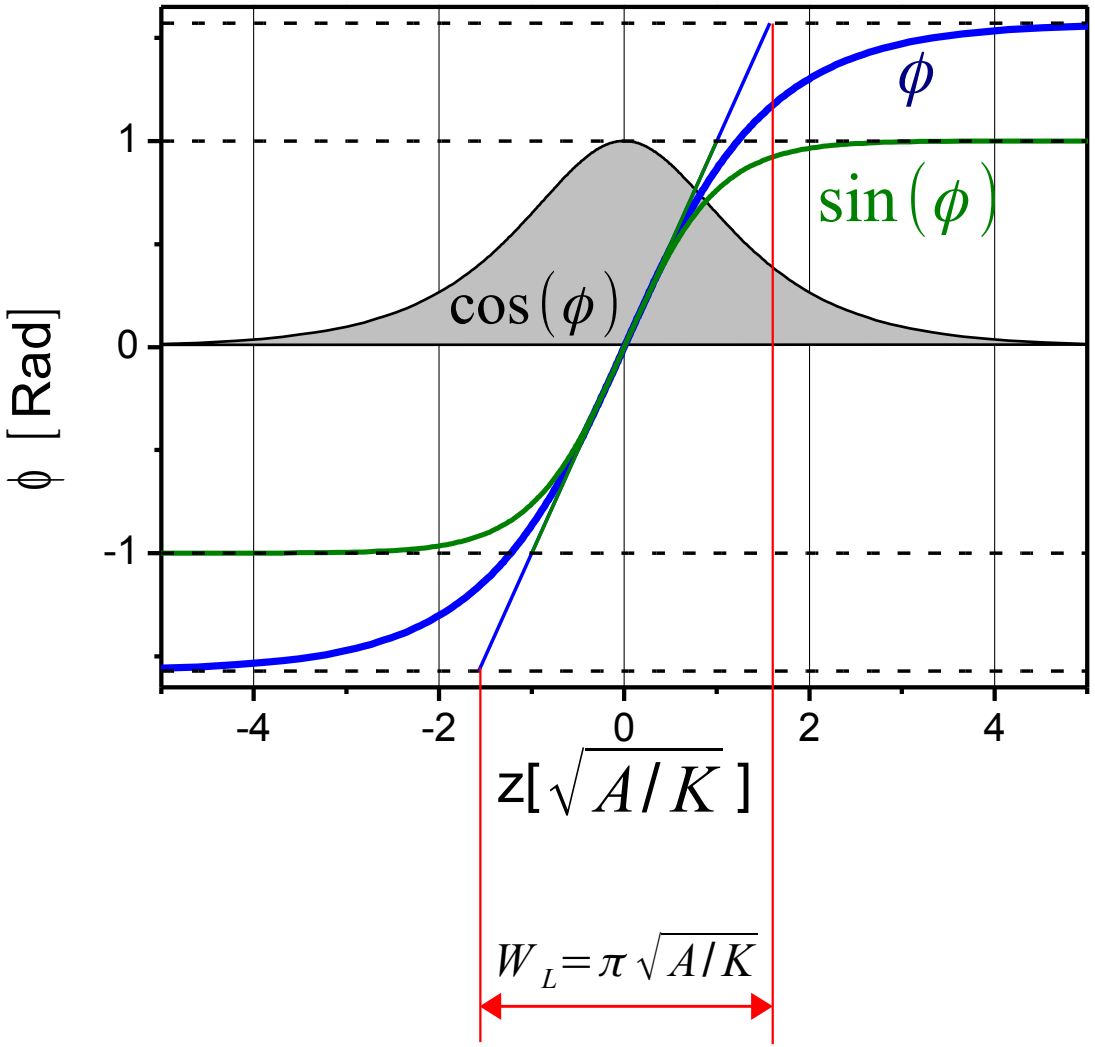

•Since the rotation of spins within Bloch wall extends to infinity there is no unique definition of its width

•Some most popular definitions:

1. Based on the slope of the φ(x) dependence for *x*=0 (Lilley):

$W_L = \pi\sqrt{A/K}$ *

2. Based on the slope of the sin(φ(x)) dependence for *x*=0:

$W_m = 2\sqrt{A/K}$

3. Integral definition:

$$W_F = \int_{-\infty}^{+\infty} \cos\phi(x)\,dx$$

- better reliability in experimental practice than the above definitions based on a single point in a profile

*most commonly used [3]

Domain walls - width

- Taking into account anisotropy constants of higher order changes the expression for domain width [4]:

$$W_L = \pi \sqrt{A l / (K_1 + K_2)}$$

- Domain width for exemplary ferromagnetic materials [4]:

	W_L [nm]	γ [10^{-2} Jm^{-2}]	
Co	22.3	1.49	
$SmCo_5$	2.64	5.71	← high anisotropy material
Sm_2Co_{17}	5.74	3.07	
$Nd_2Fe_{14}B$	3.82	2.24	
$Ni_{80}Fe_{20}$	2000*	0.01	← low anisotropy material

*J. L. Tsai, S. F. Lee, Y. D. Yao, C. Yu, and S. H. Liou, J. Appl. Phys. **91**, 7983 (2002)

Domain walls

•The minimization of **magnetostatic** and exchange energies favors planar Bloch walls in infinite or bulk samples [1].

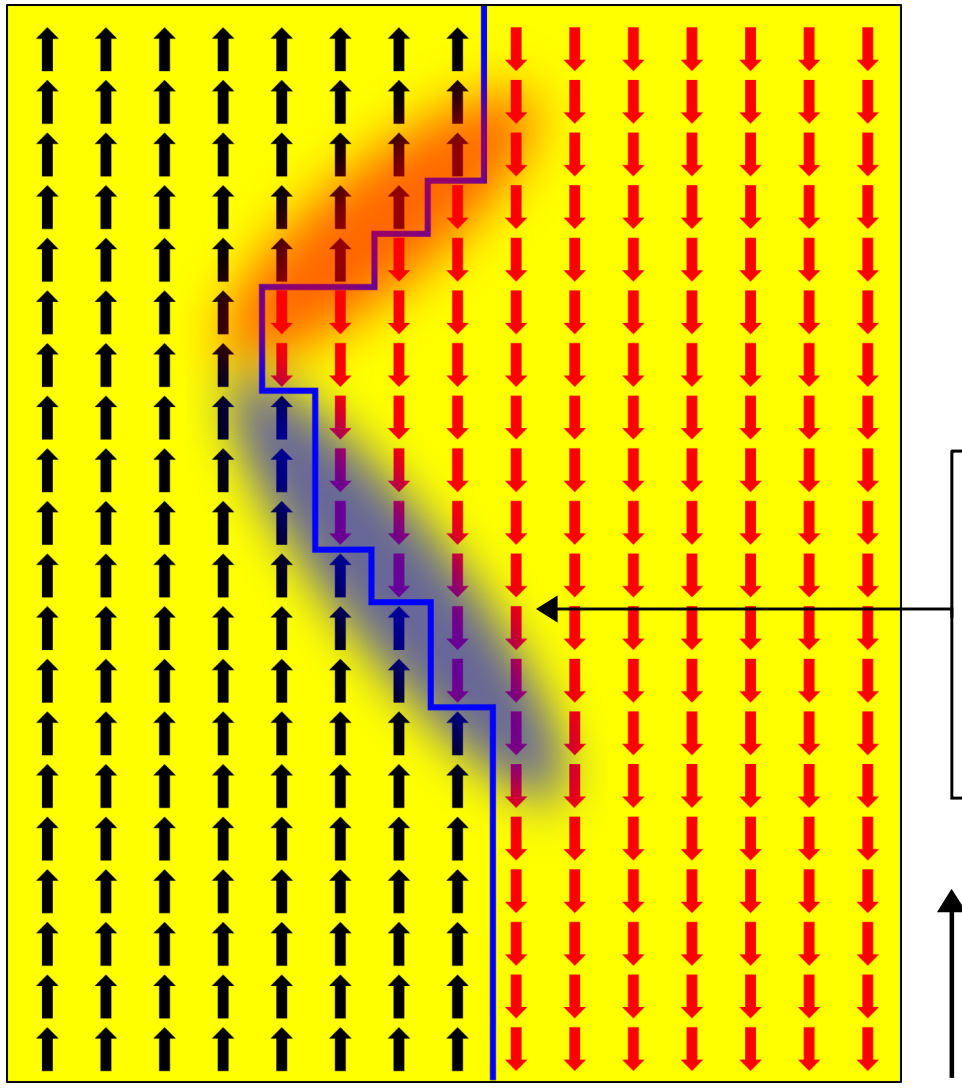

• Meandering domain wall is a source of magnetic charges

•The charges appear where the local magnetization is not parallel to domain wall

•The surface density of the charge created on the wall is:

$$\rho_{magn} = -\nabla \cdot \vec{M}\, dx = \frac{\Delta M}{dx}\, dx = -\left(\frac{-2 M_S}{dx}\, dx\right)$$

or

$$\rho_{magn} = \vec{M} \cdot \hat{n} = M_S + M_S = 2 M_s$$

Domain walls

•The minimization of magnetostatic and **exchange** energies favors planar Bloch walls in infinite or bulk samples [1]

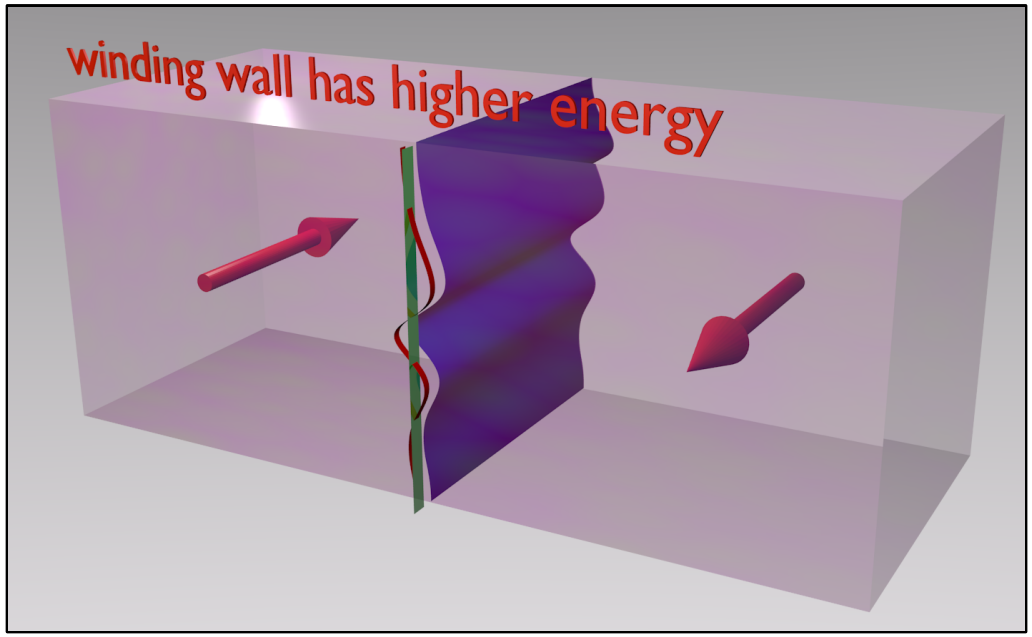

• When the wall winds in a plane perpendicular to the magnetization (see left) no magnetic charges appear

•The increased length of the wall is the source of additional exchange and anisotropy energy, though.
•The wall tends to decrease the area of its surface unless there is some reason to sustain the non-planar shape [1].

•Some of possible mechanisms are:
-presence of inclusions, voids
-internal stress
-orientation dependence of wall energy

Domain walls – pinning on narrows

•The tendency of the domain walls to minimize its length results in pinning at notches made in magnetic wires.

• NiFe(20 nm)/Cu(10 nm)/NiFe(5 nm)

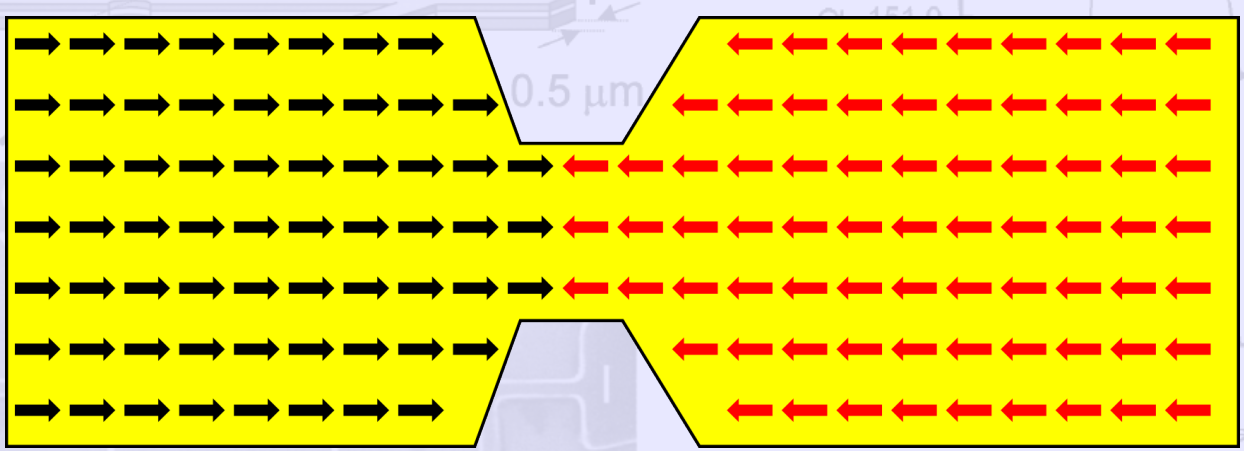

•The domain wall positioned at narrows minimizes its length and thus the energy

•To minimize magnetostatic energy the magnetic moments align along the axis of magnetic wire

•Note the presence of head-to-head domain wall

T. Ono et al., Appl. Phys. Lett., **72**, 1116 (1998)

Domain walls – pinning on narrows

- The tendency of the domain walls to minimize its length results in pinning at notches made in magnetic wires.
- NiFe(20 nm)/Cu(10 nm)/NiFe(5 nm)

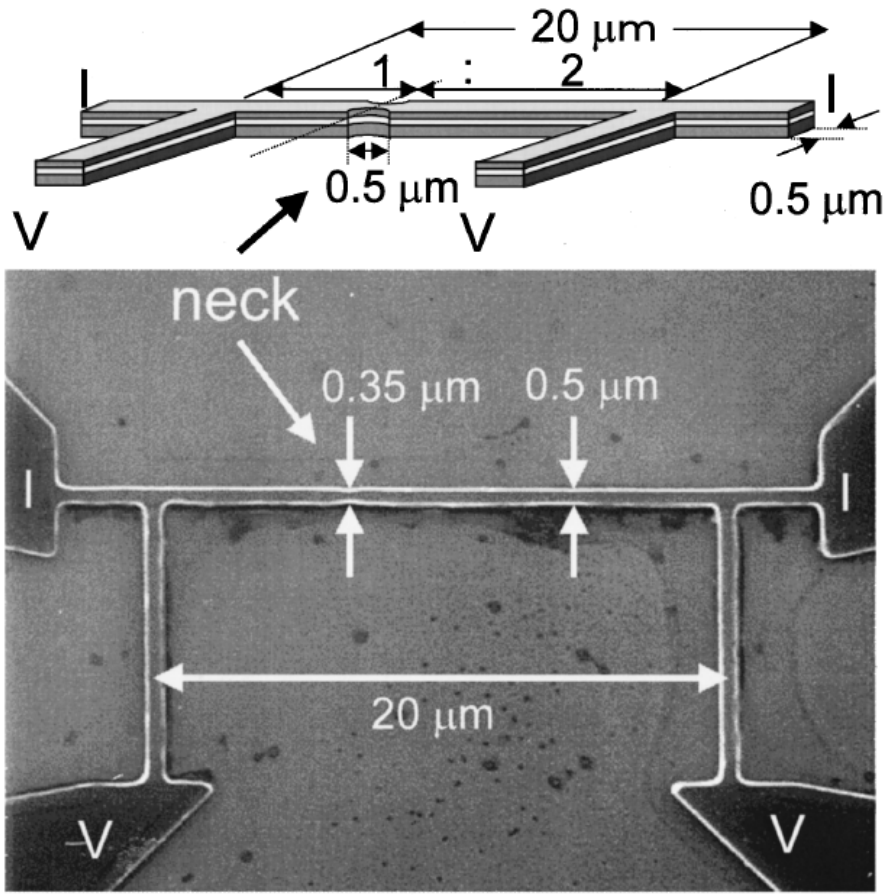

FIG. 1. SEM image and schematic illustration of the sample. The sample consists of a NiFe(200 Å)/Cu(100 Å)/NiFe(50 Å) trilayer.

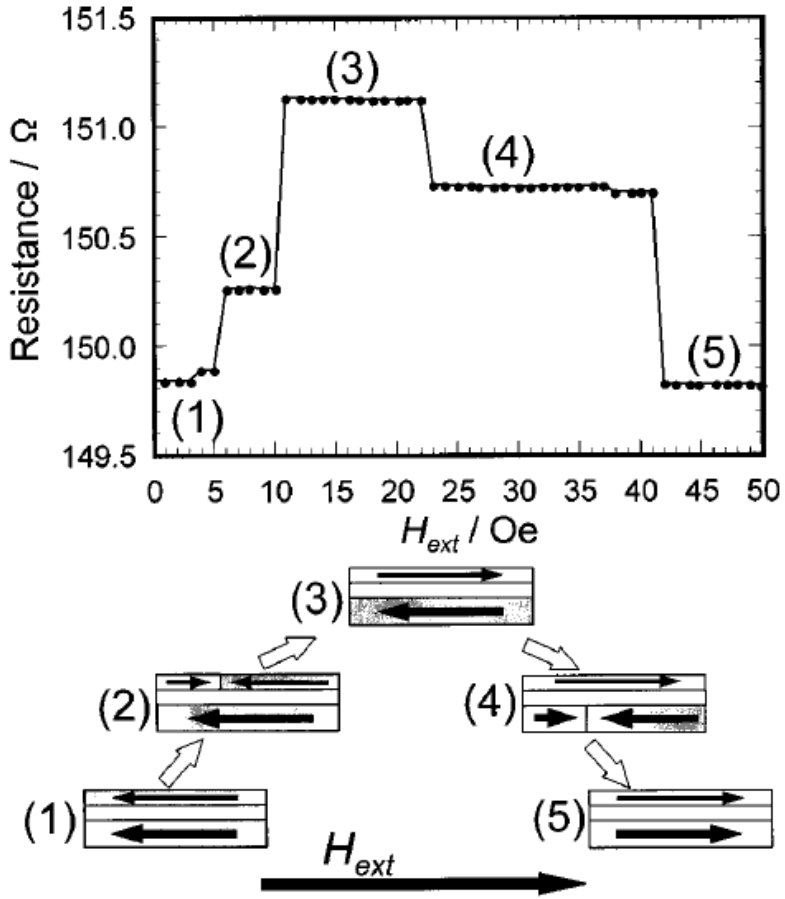

FIG. 2. Resistance as a function of the external magnetic field at 300 K determined by the four-point dc technique as illustrated in Fig. 1. The magnetic domain structures inferred from the resistance measurement and the direction of the external field are schematically shown.

T. Ono et al., Appl. Phys. Lett., **72**, 1116 (1998)

Quality factor

•It is usual in analysis of magnetic structures to define quality factor *Q* [3, p.120] which is a quotient of relevant anisotropy energy density (for example uniaxial anisotropy) and the maximum possible energy density which may be connected to stray fields:

$$Q = \frac{K_A}{K_{demag}}$$

$$K_{demag} = \frac{1}{2}\mu_0 M_S^2$$

•There are rare cases when stray field energy exceeds the value given by the expression for K_{demag} but even then the energy is proportional to K_{demag}.
•For $Q \gg 1$ the magnetization will be aligned along one of the easy directions
•The sample of infinite length and uniform cross-section easy axis (shape anisotropy) states are energetically favorable even for small Q – no domain structure is expected

Single domain particles

•There exists a critical diameter below which it is energetically more favorable for a particle to have a monodomain state [3,4].
•The gain in energy through the division into domains is less then than the energy of the domain wall between domains.

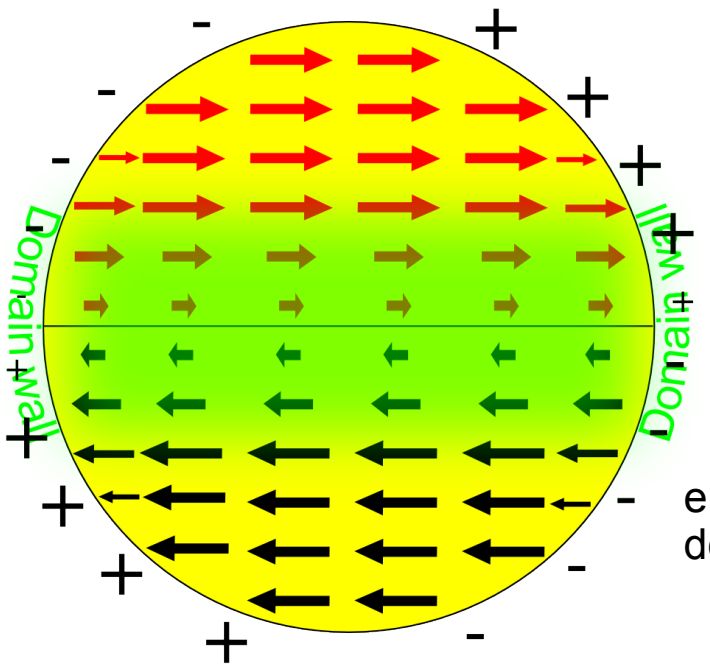

•Equating the energies of single domain cylinder with a cylinder subdivided into two domains (see 15 slides back) but with domain wall energy included we get* *per unit length* (assuming that the wall is placed in the middle of the cylinder):

$$\mu_0 \frac{\pi}{4} r^2 M_S^2 = \gamma\, 2r + \mu_0 \frac{1}{\pi} r^2 M_S^2$$

← energy of the cylinder with two domains

energy of the single domain cylinder

wall energy per unit area

•We have $\gamma = 4\sqrt{AK}$ so it follows that the critical radius is:

$$r_c = \frac{8 \cdot 4}{\pi^2 - 4} \frac{\sqrt{AK}}{\mu_0 M_s^2} \approx 17 \frac{\sqrt{AK}}{\mu_0 M_s^2}$$

*exact calculations must include size dependence of wall energy [3]

Single domain particles

•The infinite cylinder divides into domains if its radius exceeds*:

$$r_c \approx 17 \frac{\sqrt{AK}}{\mu_0 M_s^2}$$

•Calculations (still without including size dependence of DWs energy) show that for spherical particles the critical radius is [3]:

$$r_c \approx 35 \frac{\sqrt{AK}}{\mu_0 M_s^2}$$

•The critical size is shape dependent so that the analytical expressions give only the approximate values. For cubic particles the critical size is given by [3]:

$$l_c \approx 12.3 \frac{\sqrt{AK}}{\mu_0 M_s^2}$$

•The transition from two-domain to three domain configuration takes place at approximately:

$$l_c \approx 38 \frac{\sqrt{AK}}{\mu_0 M_s^2}$$

•Needle-like particles are characterized by a large critical diameter – application in recording industry [4].

*exact calculations must include size dependence of wall energy [3]

Single domain particles

- **$Sm_2Fe_{17}N_3$** particles (2 wt%) were mixed with and distributed homogeneously in a Zn metal powder matrix, and the mixture was compressed at about 20 MPa into spherical pellets about 1 mm thick.
- The 2 wt% of $Sm_2Fe_{17}N_3$ particles in the Zn matrix corresponds to an average distance of 5 times the particle diameter when the distribution is homogeneous.
- Dome-shaped particles with a critical single-domain diameter of 2 μm.
- The sample magnetization can be reversed by the 5T field (compare panels b and c)

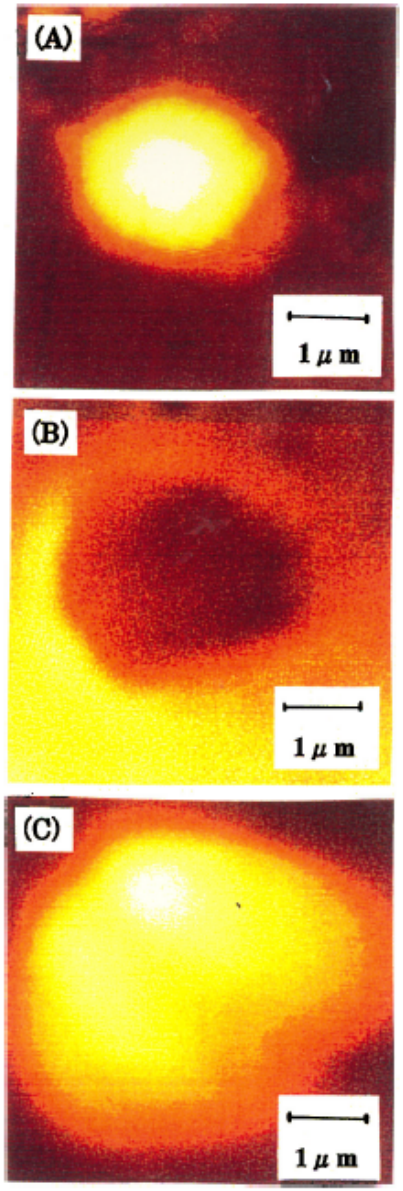

Fig. 1. Single-domain particle. (A) AFM (STM) image; (B) MFM image in demagnetized state; (C) MFM image after pulse magnetization at 5 T perpendicular to the polished surface.

KURIMA KOBAYASHI, AKIKO SAITO, and M. NAKAMURA, Electrical Engineering in Japan **154**, 1 (2006)

Single domain particles

•Magnetic states of small cubic particles with uniaxial anisotropy

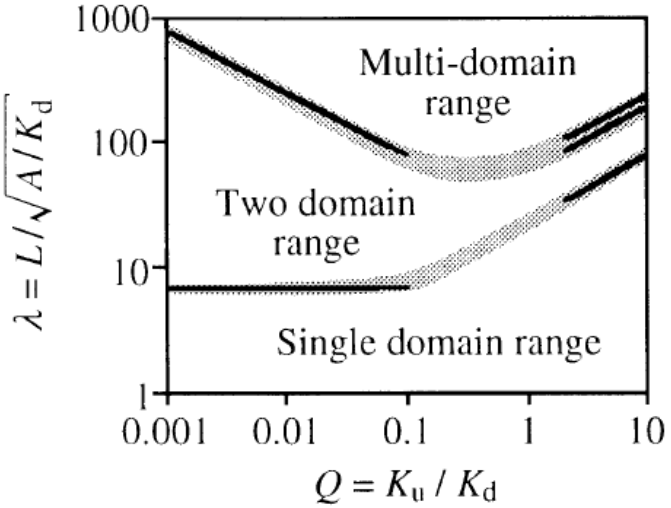

•High uniaxial anisotropy (high Q) hinders creation of magnetic domains

•All two and multi-domain configurations are not unique

Fig. 2. Sketch of the phase diagram as based on domain theory alone, using the asymptotic behavior for large and small Q derived in this section. The regions where the exact phase boundaries are anticipated are indicated by the gray shaded areas.

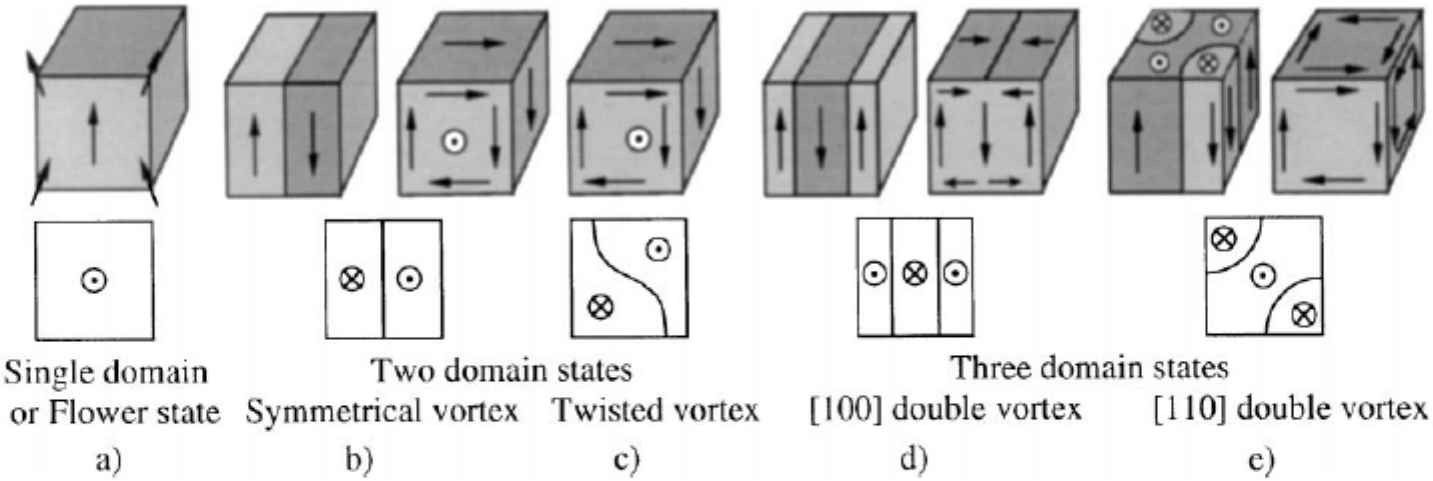

Fig. 14. The energetically favored one, two and three-domain states: (a) flower state, (b, c) two-domain states for high and low anisotropy, (d, e) three-domain states for high and low anisotropy. The sketches in the second row always show the central slice in the z-direction indicating the walls and domains.

W. Rave, K. Fabian, A. Hubert, JMMM 190, 332 (1998)

Single domain particles

•Critical sizes of spherical particles [4] according to expression: $r_c \approx 36 \frac{\sqrt{AK}}{\mu_0 M_s^2}$

	r_c[nm]	γ [10^{-3} Jm^{-2}]
α-Fe	5.8	2.1
Co	27.8	7.84
Ni	11.3	0.39
Fe_3O_4	6.2	2.0
CrO_2	90	2.0
$SmCo_5$	585	57

◄— low anisotropy material

◄— high anisotropy material

•Critical radii of spherical magnetic particles are typically of the order of 10 -100 nm. For iron single-domain particle may contain up to about 35×10^3 atoms and for $SmCo_5$ over 1×10^{10} atoms.

Domain configuration in nanorings

- Shape of the particles has great influence on their magnetic properties.
- For cubic or spherical particles one can define the size limit by single number but for complex shapes more parameters are needed.
- The treatment is limited to single domain size, uniaxial anisotropy, and only three particular magnetization states are considered: **uniform in-plane, uniform axial, and vortex**.

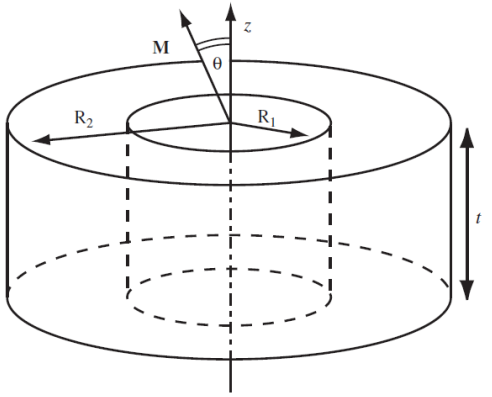

Fig. 1. Schematic representation of a ring shaped object with rectangular cross-section. In general, the magnetization **M** forms an angle θ with the z axis. For the two configurations studied, we have $\theta = 0$ (axial) and $\theta = \pi/2$ (in-plane).

$$\sigma = \frac{R_1}{R_2}$$

$$\tau = \frac{t}{2R_2}$$

$$\varepsilon = -\frac{K_u}{K_d}$$

$$\gamma = \frac{2\sqrt{A/K_d}}{R_2^2}$$

uniform axial, (**M** parallel to *z* axis)

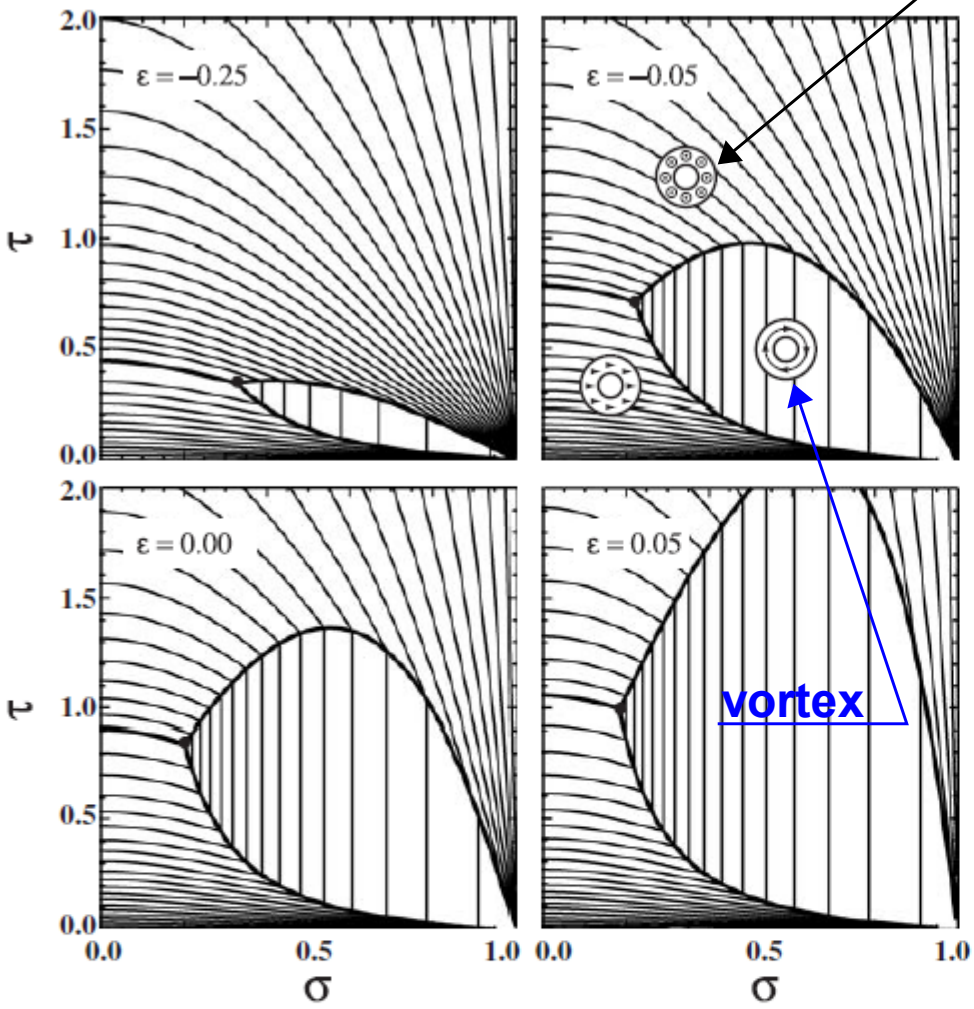

Fig. 4. Phase diagrams of the magnetized ring as a function of the shape parameters σ and τ for fixed value of $\gamma = 0.2$ and several values of ε. The vortex region grows rapidly with increasing ε.

M. Beleggia et al., Journal of Magnetism and Magnetic Materials **301**, 131 (2006)

Domain configuration in nanorings

- Permalloy nanoring:

$R_1 = (58 \pm 5)\ nm$

$R_2 = (104 \pm 5)\ nm$

$t = (4.7 \pm 0.8)\ nm$

- Electron holography confirms **vortex state** in nanoring

- The magnetization in vortex state is “single domain” as there are no abrupt changes of magnetic moment direction within the ring

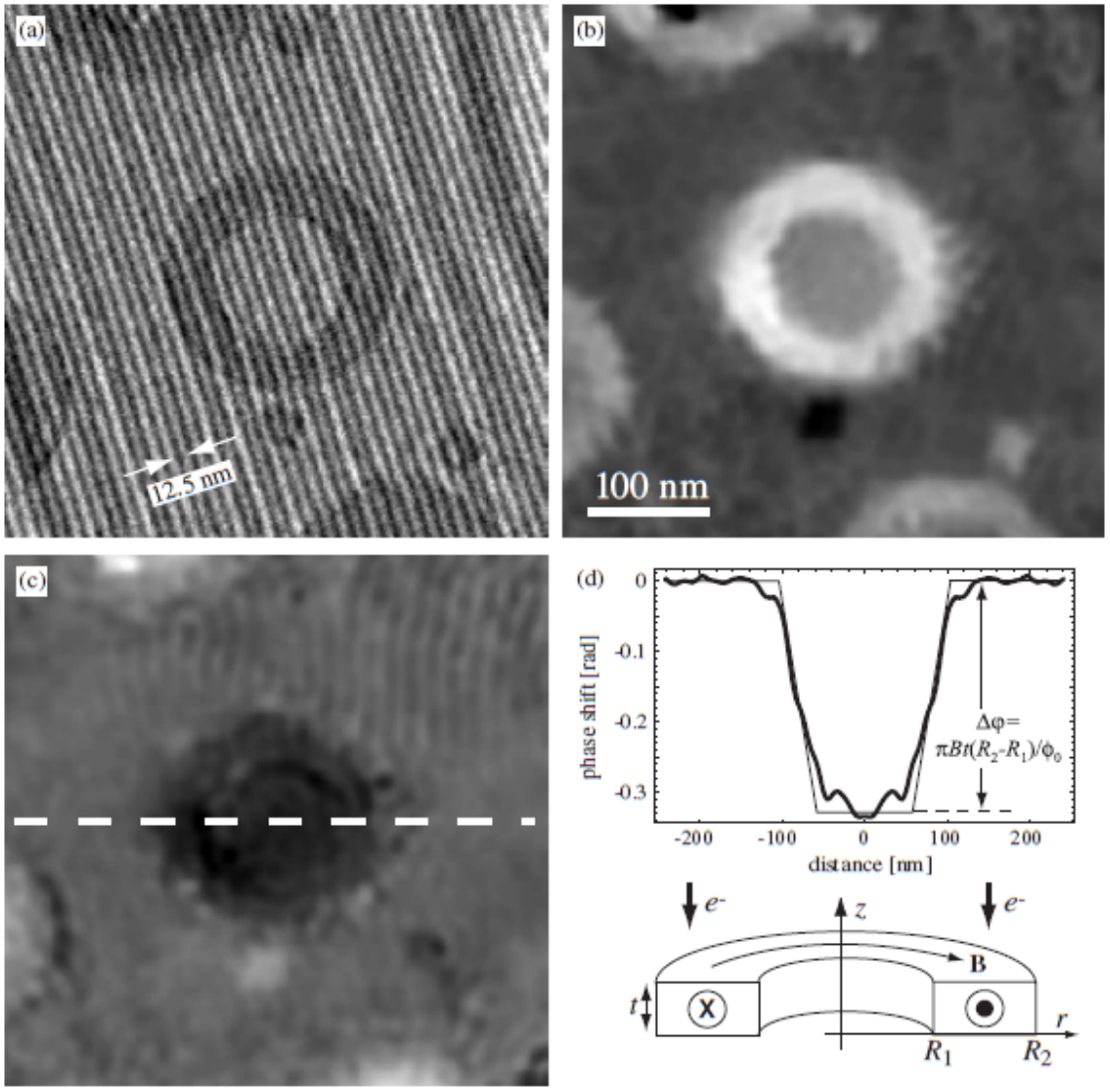

Fig. 11. (a) Hologram of a permalloy ring ($\tau \simeq 0.023$, $\sigma \simeq 0.55$) on amorphous Silicon Nitride membrane. The interference fringes have an average spacing of 12.5 nm. (b) Reconstructed electron phase shift showing total contribution from electric and magnetic components. (c) Magnetic component of phase shift obtained from the difference of reconstructed phase maps obtained after flipping the sample 180° relative to the electron beam. (d) Average profile along dashed line in (c) showing the magnetic phase shift consistent with a ring in the vortex state. A phase simulation from an ideal ring of the specified sizes and with a magnetic field of 1 T is superimposed to the experimental profile as a thin line. The total phase difference $\Delta\varphi$ is proportional to the ratio between the total magnetic flux in the ring cross-section and the flux quantum ϕ_0.

M. Beleggia et al., Journal of Magnetism and Magnetic Materials **301**, 131 (2006)

Superparamagnetic particles

•The uniaxial anisotropy particle of volume V has the anisotropy energy given by:

$$E_A = V K \sin^2\theta$$

•To change the direction to the opposite one along easy axis (from red to yellow arrow, to the right) the magnetic moment has to overcome the energy barrier equal to the maximum anisotropy energy:

$$\Delta E = V K$$

•The energy can be provided by the external field but if the particle is small enough the thermal fluctuation energy may be enough to overcome the barrier [5].
•If K=0 then the moment can point in any direction with equal probability and the classical theory of paramagnetism applies (see lecture 3).
•The essential difference though is that the magnetic moment of the particle may be much higher than that of typical paramagnetic atom or ion which is usually few μ_B [5].
•5 nm iron sphere (much smaller than single-domain critical diameter!) has moment of about $5560 \times 2.2 = 12{,}000\ \mu_B$.

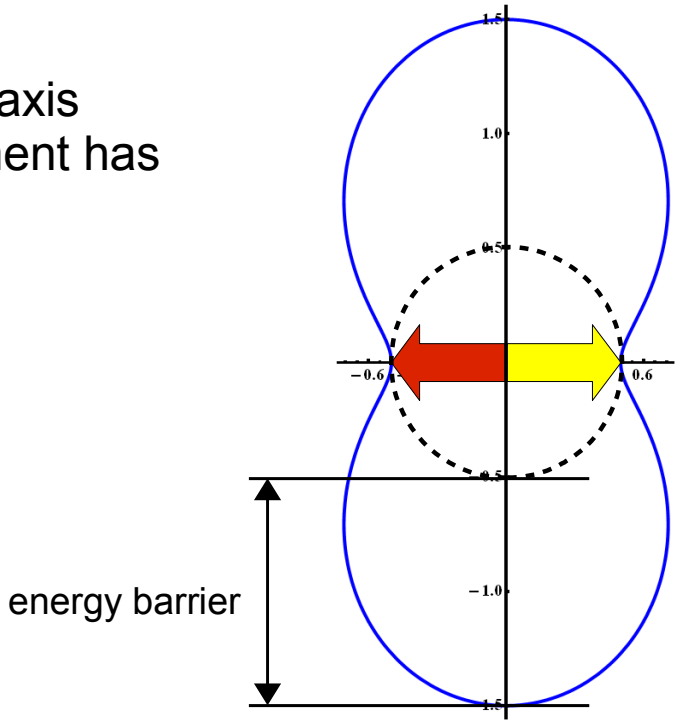

For spherical particles of cubic structure the energy barrier between neighboring stable directions is kV/4 if easy directions are <100> and KV/12 if easy directions are <111>.

Superparamagnetic particles

•As a result of high moments the assembly of superparamagnetic particles saturates in relatively weak external fields:

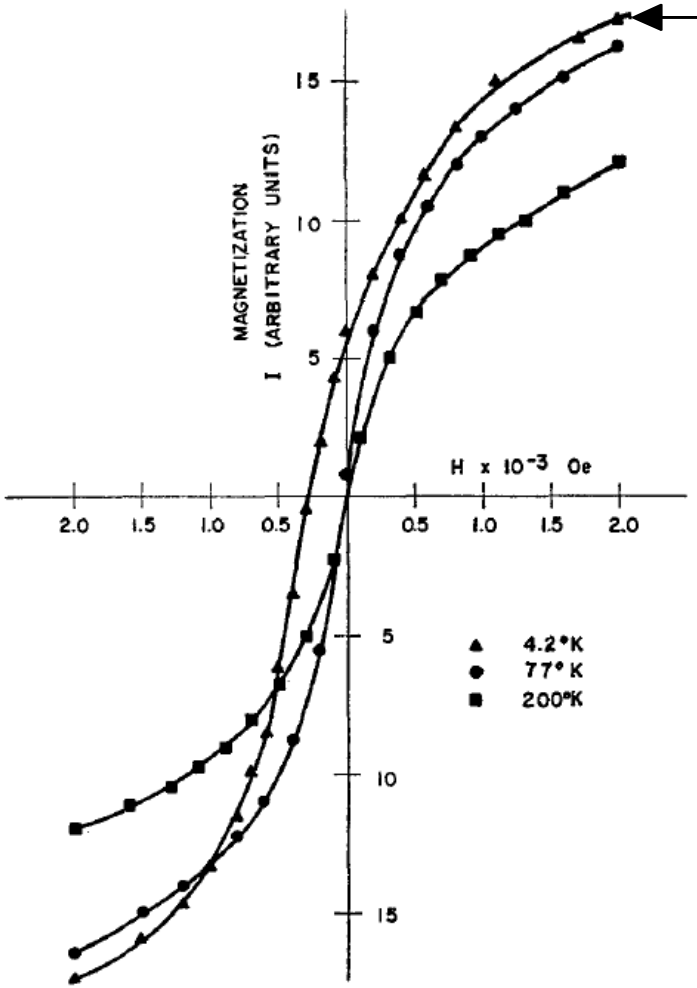

this curve is not "superparamagnetic"

FIG. 1. Low field portion of demagnetization curves of fresh iron amalgam. This amalgam consists of 2% iron by volume in the form of small iron particles whose diameters are estimated to lie between 30 A and 45 A.

C. P. Bean and I.S. Jacobs, J. Appl. Phys. **27**, 1448 (1956)

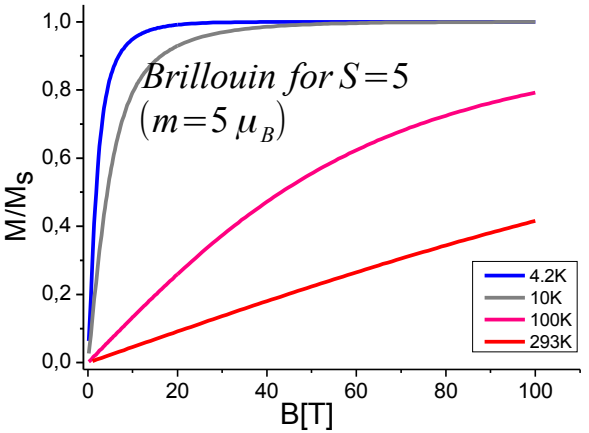

$$\frac{\langle S_z \rangle}{S} = B_S\left(\frac{g\,\mu_B S\,B}{k_B T}\right)$$

•**Very high moments *S*** of superparamagnetic particles results in saturation in much weaker fields

•Technical saturation can be reached even at room temperature

$$B_S(x) = \frac{2S+1}{2S}\coth\left(\frac{2S+1}{2S}x\right) - \frac{1}{2S}\coth\left(\frac{x}{2S}\right)$$

Superparamagnetic particles

•As seen on previous slide the superparamagnetism disappears below critical blocking temperature T_B.

•We assume that the external field magnetized the sample to initial magnetization $\boldsymbol{M}_i$ and was turned off at t=0 [5]. The magnetization will start do decrease with a rate depending on temperature and $\boldsymbol{M}_i$. The time dependence may be approximated by:

$$\frac{dM}{dt} = f_0 M e^{-KV/k_B T} \equiv \frac{M}{\tau} \qquad with \qquad \frac{1}{\tau} = f_0 e^{-KV/k_B T}, \quad f \approx 10^9 Hz$$ - frequency factor

•Integrating we get:

$$M_R = M_i e^{-t/\tau}$$

•The relaxation time is very strongly dependent on V and T:

Spherical Co particle	
6.8 nm diameter	9 nm diameter
τ=0.1 s	τ=3.3×10^9 s (100 yers)

•The assembly of 9 nm particles is essentially stable with respect to magnetization at RT [5]

Superparamagnetic particles

•The dependence of the relaxation time τ on V/T quotient is used for the *arbitrary definition of superparamagnetic limit*, i.e., the size of the particle below which the resultant magnetic moment the assembly of them is unstable:
The critical value of relaxation time is arbitrarily taken to be 100 s [5]**.**

•It follows from $\frac{1}{\tau} = f_0 e^{-KV/k_B T}$ that for τ =100 s:

$$KV/k_B T = 25$$

•The transition from “stable” to “unstable” behavior for uniaxial particles takes place at roughly:

$$V_{sp} = \frac{25 k_B T}{K}$$

this value has only accessory character

•For spherical Co particle the critical diameter is 7.6nm at RT.

•It should be noted that the superparamagnetic character of the assembly of particles depends on the time scale of the experiment used for its investigation.

Superparamagnetic particles – blocking temperature

•The assembly of small particles of a constant size will have a stable magnetization (τ=100 s). For uniaxial particles and the same as above criterion of stability we have [5]:

$$T_b = \frac{KV}{25 k_B}$$

•Schematic representation of the behavior of single domain particles versus temperature:

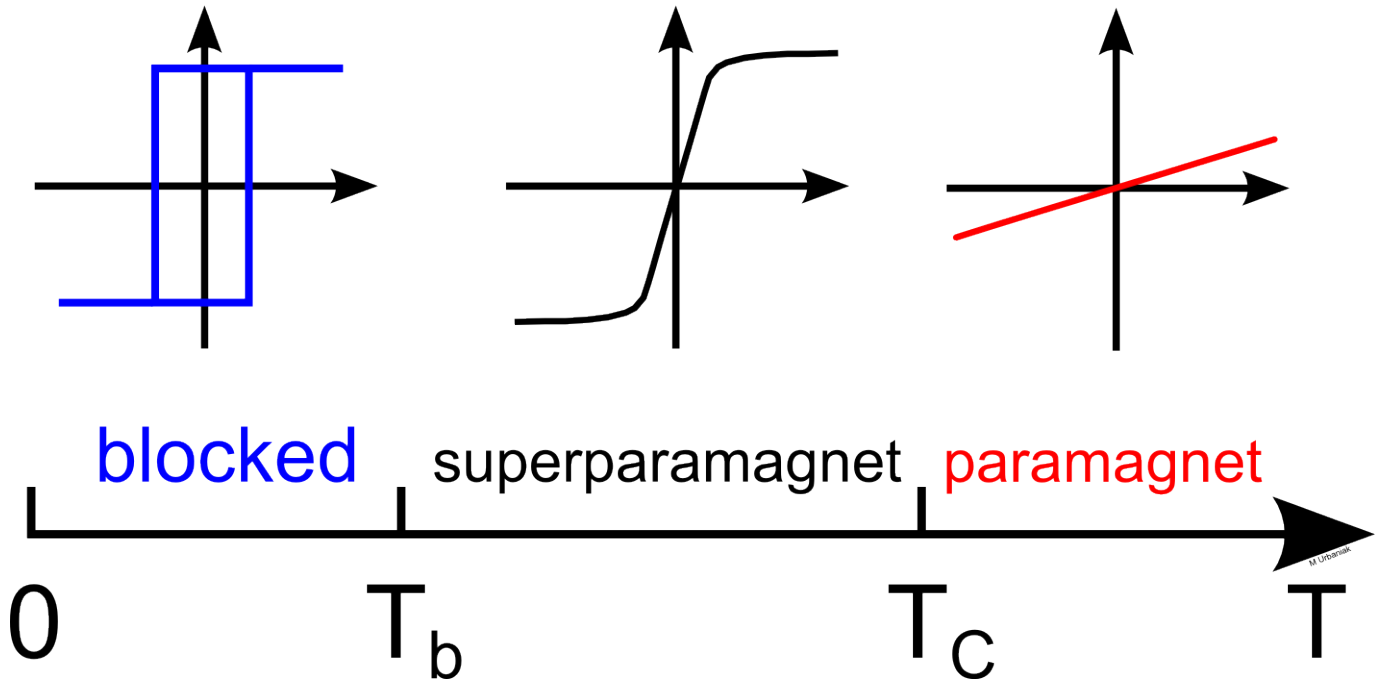

*graphics based on Fig.8.30 from [6]: J.M.D. Coey, Magnetism and Magnetic Materials, Cambridge University Press 2009

Superparamagnetic particles – coercive field

•The energy of the uniaxial anisotropy particle in field ***B* parallel** to *z* axis (easy axis) is [5]:

$$E = V\left(K\sin^2\theta - BM\cos\theta\right)$$

•The effect of the external magnetic field on the assembly of single-domain particles is to change energy barrier:

$$\frac{\partial E}{\partial \theta} = V\left(2K\sin\theta\cos\theta + BM\sin\theta\right)$$

$$\frac{\partial E}{\partial \theta} = 0 \rightarrow \cos\theta_{max} = -\frac{M}{2K}B$$

$$E\left(\theta_{max}\right) = VK\left[1 - \left(\frac{M}{2K}B\right)^2\right] + \frac{B^2M^2V}{2K}$$

$$\Delta E = E\left(\theta_{max}\right) - VBM$$

$$\Delta E = KV\left(1 - \frac{BM}{2K}\right)^2$$

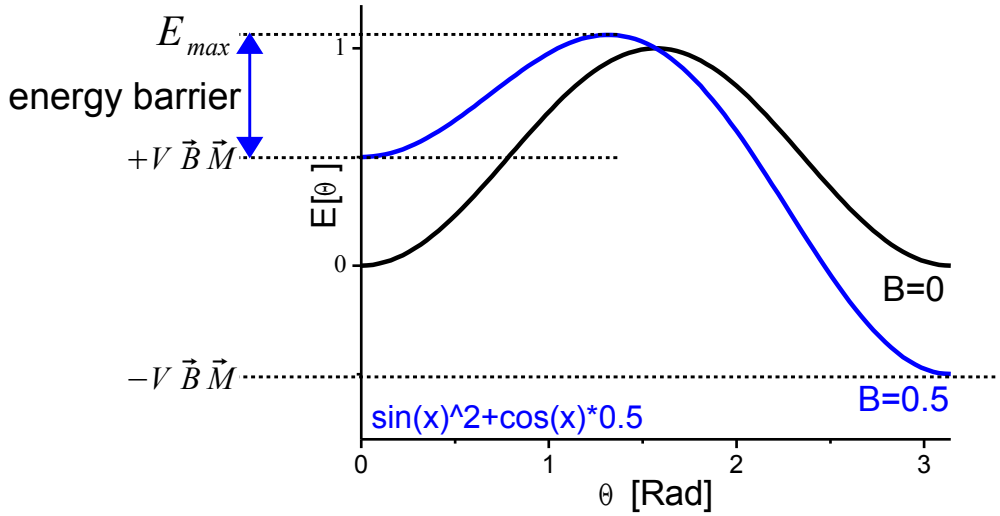

Superparamagnetic particles – coercive field

•The energy of the uniaxial anisotropy particle in field ***B* parallel** to *z* axis (easy axis) is [5]:

$$E = V\left(K\sin^2\theta + BM\cos\theta\right)$$

•The effect of the external magnetic field on the assembly of single-domain particles is to change energy barrier:

$$\Delta E = K V\left(1-\frac{B M}{2\mathrm{K}}\right)^2$$

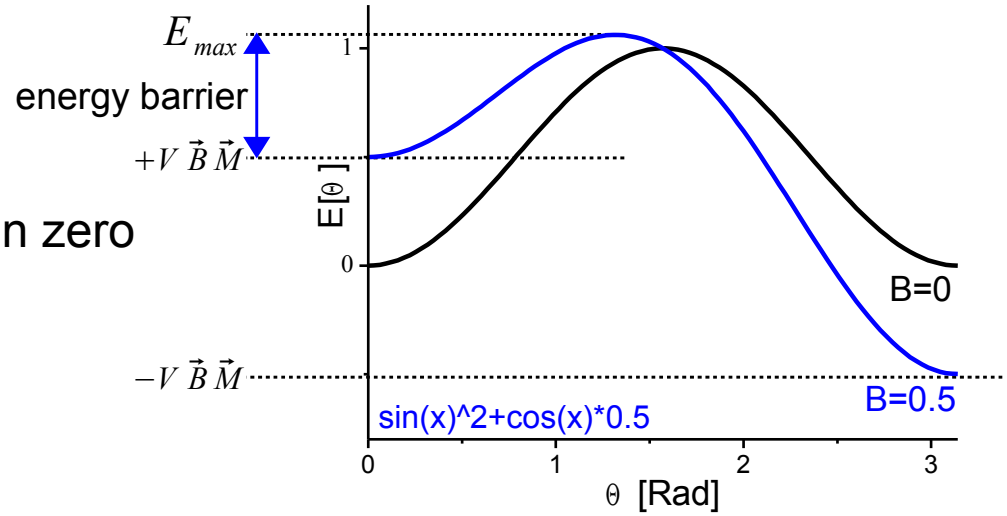

•The particle of a given size which was stable in zero field can become unstable in external field. As previously, for τ=100 s, we get:

$$\Delta E = K V\left(1-\frac{B M}{2\mathrm{K}}\right)^2 = 25 k_B T$$

•The solution is [5]:

$$H_C = \frac{1}{\mu_0}\frac{2K}{M}\left[1-\left(\frac{25 k_B T}{K V}\right)^{1/2}\right]$$

- field for which energy barrier diminishes to $25k_bT$

Superparamagnetic particles – coercive field

•For **low temperature or high volume of the particle** the expression gives the coercivity (saturation field) equal to the value when the field is unaided by thermal energy (compare Stoner-Wohlfarth model):

$$H_C = \frac{1}{\mu_0}\frac{2K}{M} \quad \Leftarrow \quad H_C = \frac{1}{\mu_0}\frac{2K}{M}\left[1-\left(\frac{25\,k_B T}{K\,V}\right)^{1/2}\right]$$

$$V_{sp} = \frac{25\,k_B T}{K}$$

$$H_C = H_{C.0}\left[1-\left(\frac{V_{sp}}{V}\right)^{1/2}\right] = H_{C.0}\left[1-\left(\frac{D_{sp}}{D}\right)^{3/2}\right]$$

•The coercivity of the assembly of superparamagnetic particles increases as the temperature is increased.
•Similar expression can be obtained for temperature dependence of coercive field. In general however the variations of H_c are due to thermal variations of anisotropy and saturation magnetization.
•In real systems there is a dispersion of particle sizes and random orientation of easy-axes.

Superparamagnetic particles – coercive field

•Coercive field of Ni powder:

$$H_C = H_{C.0}\left[1-\left(\frac{T}{T_B}\right)^{1/2}\right]$$

•Hysteresis of granular CuCo alloy:

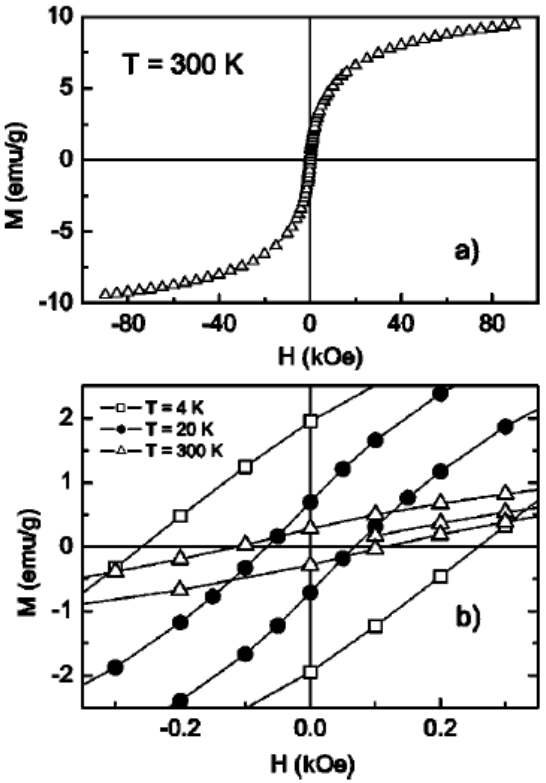

FIG. 2. (a) Hysteresis loop for the $Cu_{90}Co_{10}$ as cast sample at room temperature. (b) A detail of the narrow hysteresis at different temperatures.

W. C. Nunes, W. S. D. Folly, J. P. Sinnecker, and M. A. Novak, PHYSICAL REVIEW B **70**, 014419 (2004)

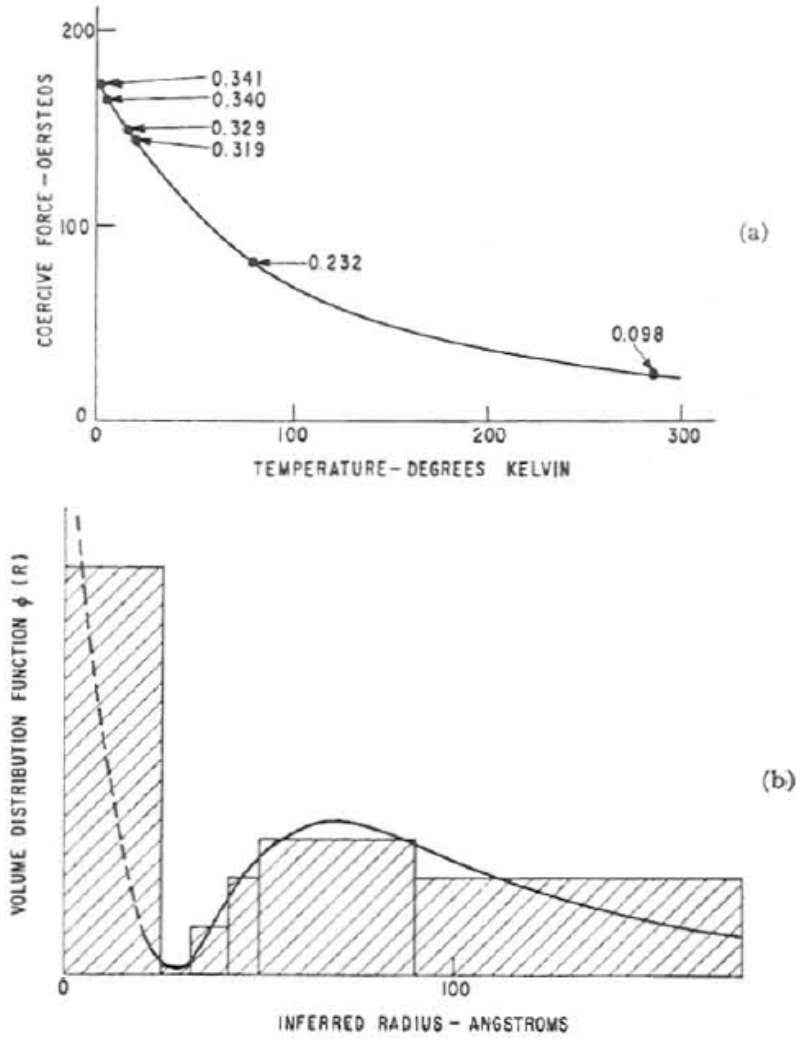

FIG. 8. (a) Coercive force *vs* temperature for a nickel powder. Numbers along the curve indicate the ratio of remanence to saturation magnetization at the various temperatures. (b) Particle size distribution inferred from these data (after Weil).

C. P. Bean and J. D. Livingston, J. Appl. Phys. **30**, S120 (1959)

Domain wall displacement

•When magnetic field is applied to ferromagnetic substances the domain structure changes as to minimize the energy: the torque/force acts on individual atomic moments as long as the reach the state in which the resultant torque is zero:

$$\vec{N} = \vec{m} \times \vec{B}_{total} = 0$$

where $\vec{B}_{total}$ is the effective field due to external field, demagnetizing field, magnetocrystalline anisotropy etc.

•When the field is applied parallelly to the magnetization of one of the domains the moments within that domain and the domains with opposite magnetization experience no torque as they are parallel to ***B***.
•Only magnetic moments located within the domain wall make an angle with ***B***:

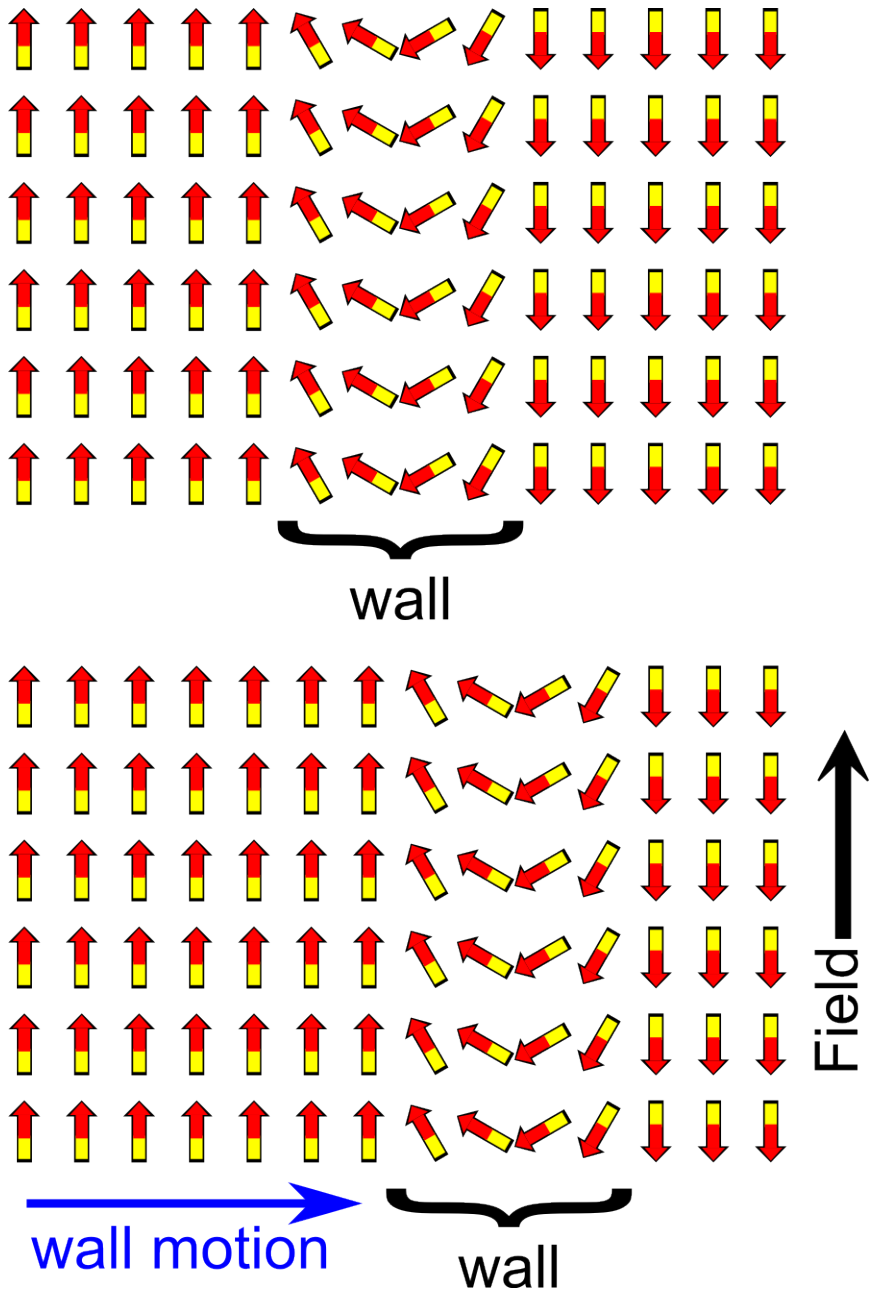

for better viewing Néel-type, not Bloch, wall is shown

graphics is a derivative work from Fig. 6.17 of [1]: S. Chikazumi, Physics of Magnetism, John Wiley & Sons, Inc., 1964

Domain wall polarization

- Depending on the sense of rotation of the magnetic moments within the domain wall most of domain walls can occur in two equivalent forms [3,5].
- A **Bloch line** is a dividing line between wall segments of different sense of rotation.
- Similarly in systems with Néel-type walls (see next lecture) one may use the term **Néel line**.
- Bloch lines can influence wall motion in a drastic way [5].

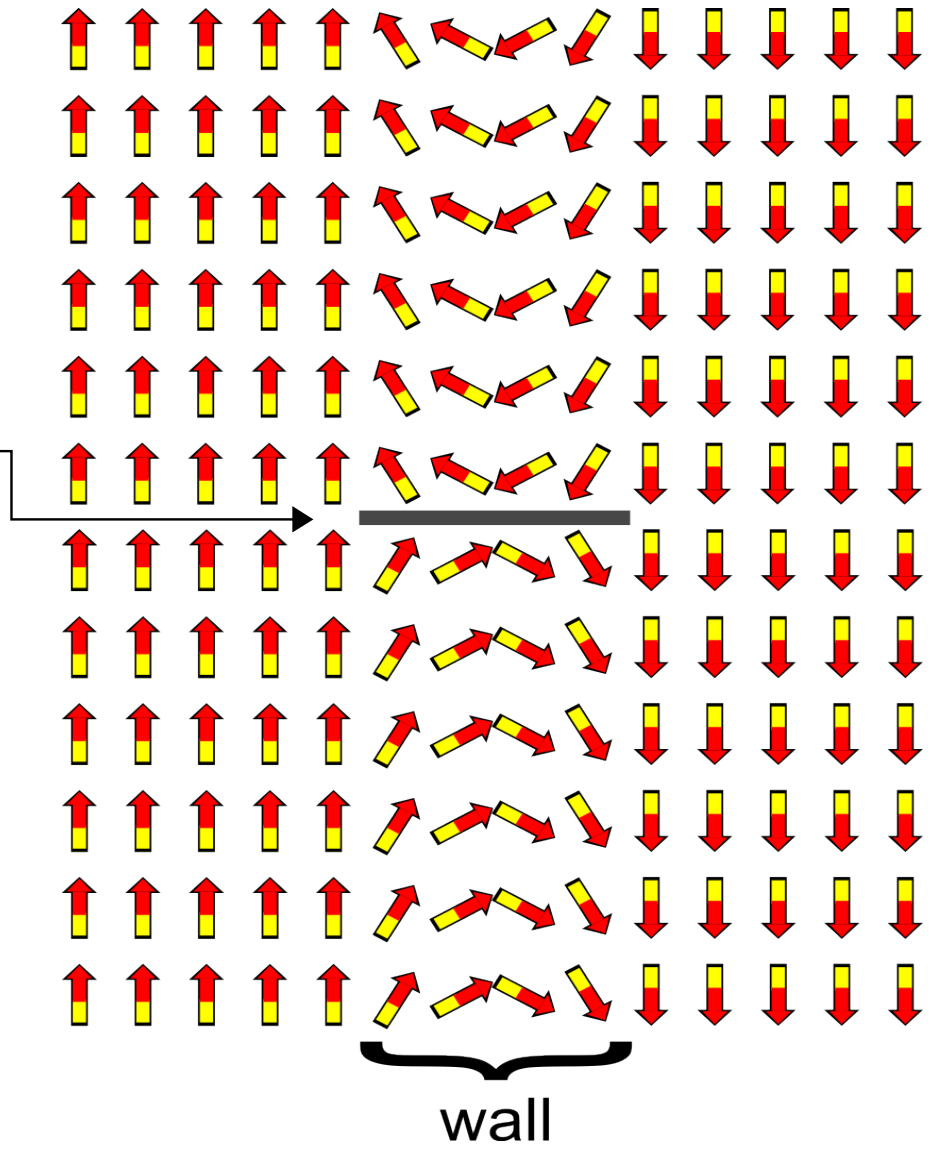

for better viewing Néel-type, not Bloch, wall is shown

Hysteresis – general classification of magnetization mechanisms

•The initial magnetization curve and the demagnetization curve can be schematically sketched as [1,5,6]:

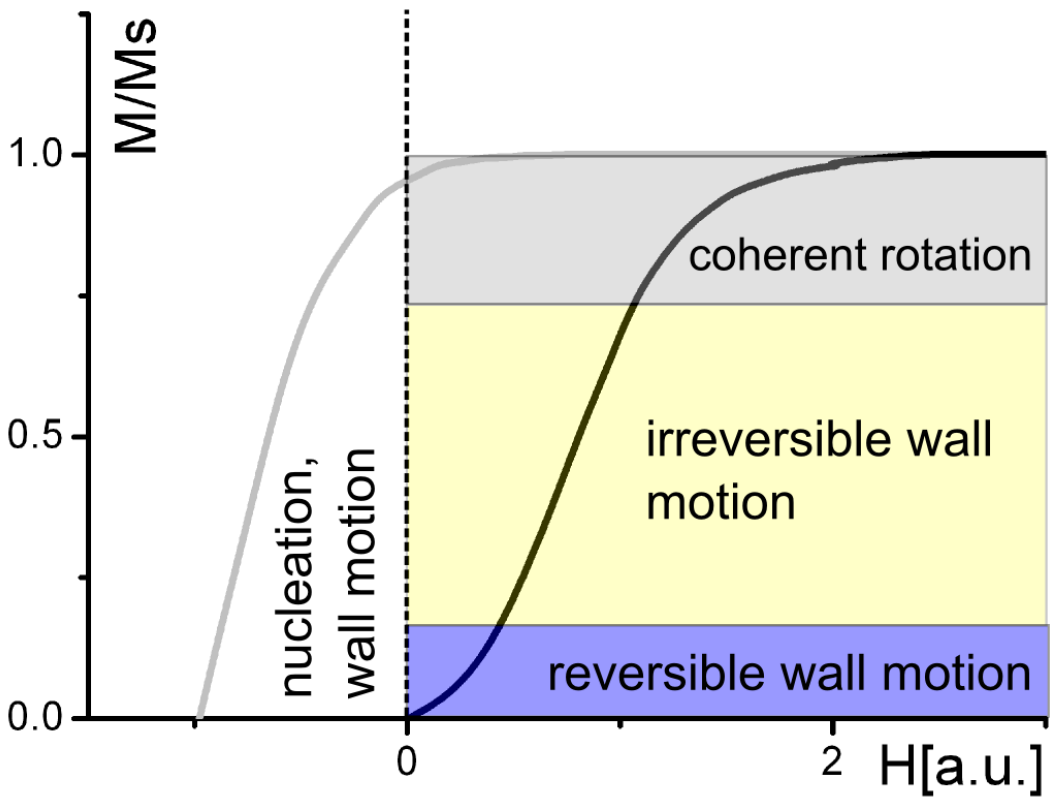

•It is not always possible to attribute precisely the field ranges to different reversal mechanisms

•Especially in magnetically hard materials wall displacement and rotation magnetization can coexist [1]

•At higher frequencies domain wall movement is more easily damped than the magnetization reversal [1].

•The region corresponding to $0.9<M/M_S<1$ is called the approach to saturation [1,6]

Domain walls and hysteresis

•Consider a uniaxial anisotropy substance which has an isotropic distribution of easy axes (polycrystalline materials) [1].
•The field dependence of the angular dependence of magnetization directions of magnetic domains can be schematically sketched as:

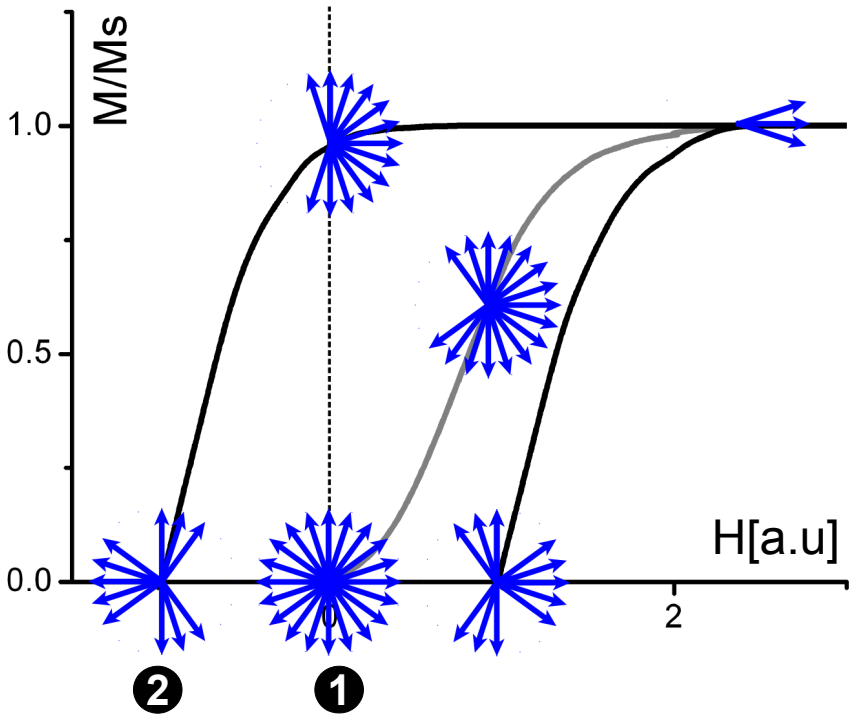

•In demagnetized state all accessible domain orientations are equally occupied

•On increasing the field the energetically favored domains (with magnetization roughly parallel to the applied field) spread over the volume of the sample.

•At technical saturation there is a limited number of domains and all moments are nearly parallel to field direction.

•The domain distributions at points 1 and 2 different although both correspond to the absence of macroscopic magnetization.

Hindrances to domain wall motion

- In real materials a nonzero applied field is necessary to move the domain wall [5].
- Crystal imperfections may hinder the motion of the wall.
- Some of imperfections result in regions of different, than the rest of the material, spontaneous magnetization – these are called *inclusions.*
- Inclusions may take many forms [5]: impurities, oxides, sulphides etc., holes, cracks...
- The most straightforward mechanism of domain pinning by the inclusion is the minimization of the wall energy by decreasing its area:

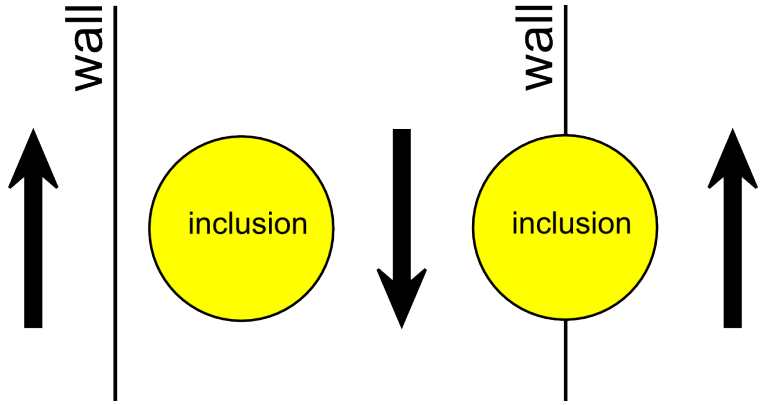

- When the wall bisects the spherical inclusion of radius *r* its surface diminishes and the wall energy related to its surface decreases by:

$$\Delta E = \pi r^2 \gamma$$

Hindrances to domain wall motion

•Néel pointed out that the appearance of surface charges on the inclusion can be lead to much greater decrease of magnetostatic energy than the change of energy related to surface change [5]:

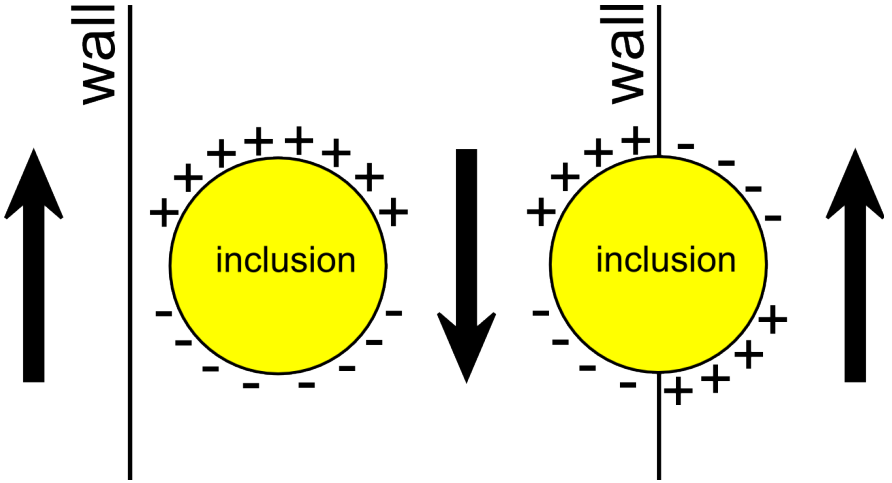

•The magnetostatic energy of the uniformly magnetized sphere is [compare p. 14]:

$$E_{demag}^{one\ domain} = \frac{1}{2} N_d M_s M_s V_{sphere} = \frac{8}{9} \pi^2 M_s^2 r^3$$

•The magnetostatic energy of sphere bisected by the wall is approximately half of the above value [5].

•The quotient of the energy gain by the virtue of magnetic charges and the gain by the decrease of the wall area is:

$$\Delta E_{charges} / \Delta E_{area} = \frac{8}{9} \frac{\pi M_s^2}{\gamma} r \quad \propto \quad r$$

For 1 μm diameter inclusion in iron the quotient is **140!**

The wall-area effect in hindering wall motion is negligible for large inclusions

Hindrances to domain wall motion

both images from H. König, Naturwissenschaften **41**, 341 (1954)

•Often the energy of the inclusion can be further reduced by the creation of additional *spike domains* protruding from it [5]:

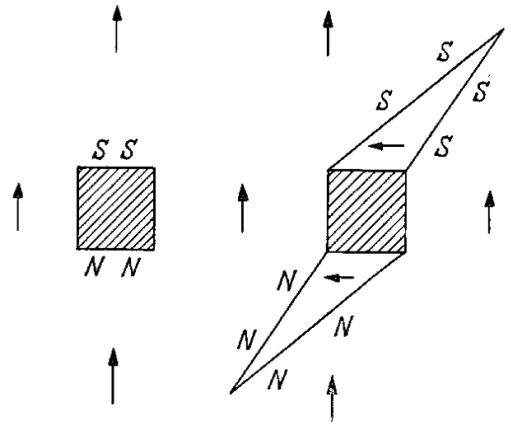

Fig. 12. Links: Freie Pole an einem kubischen Einschluß. Rechts: Vermeidung der Streufelder durch angesetzte dreieckige Zwickel nach NÉEL.

•The spikes, predicted by Néel, were first observed by H.J. Williams* in single crystal silicon-iron [on electrolitically polished (100) surface]:

•If the domain walls of spike domains were all exactly at 45^{o} to the magnetization of the surrounding domain there would be no magnetic charges
•To achieve this the wall would have to extend to infinity increasing wall surface energy
•The observed length of spikes is a compromise between this two energy contributions.

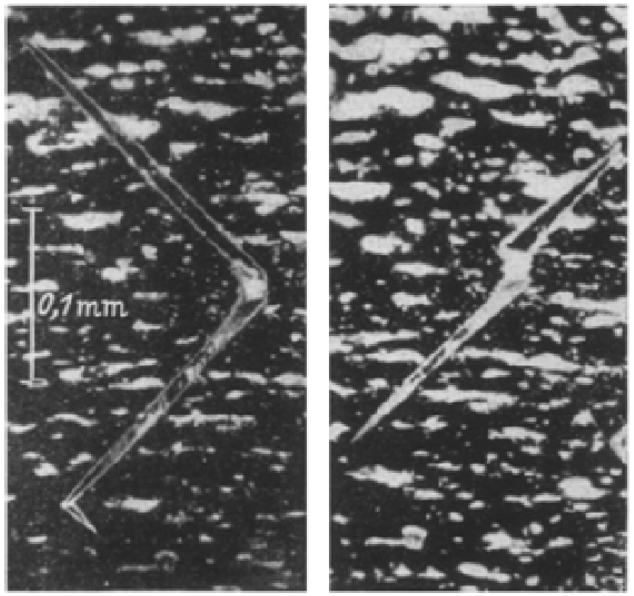

Fig. 13. Zipfelmützenförmige Elementarbereichbildung um kleine Einschlüsse. H. J. WILLIAMS.

*H.J. Williams, Phys.Rev. **71**, 646 (1947)

Hindrances to domain wall motion

•Often the energy of the inclusion can be further reduced by the creation of additional *spike domains* protruding from it [5]:

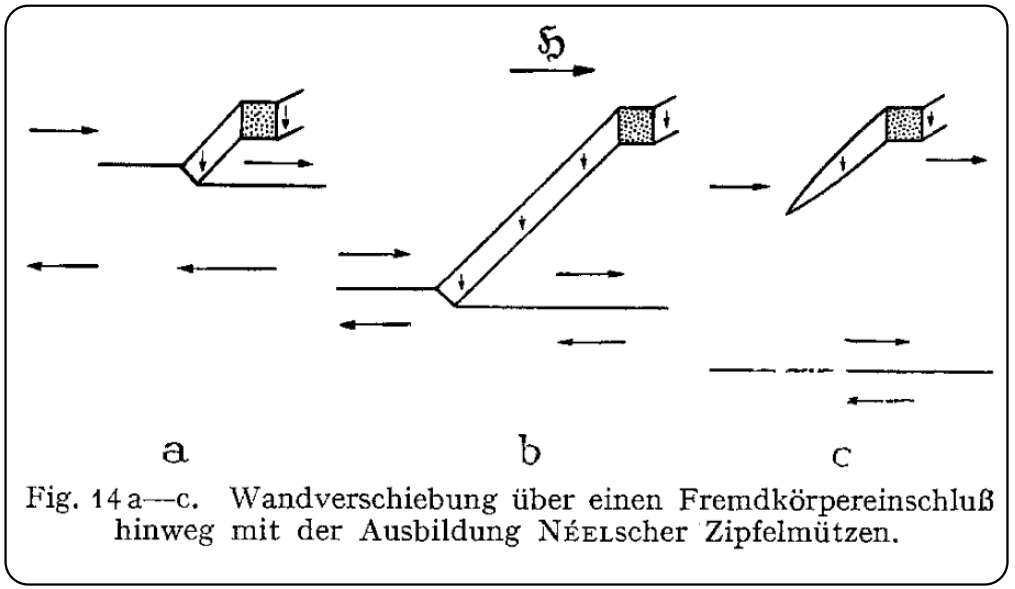

Fig. 14 a—c. Wandverschiebung über einen Fremdkörpereinschluß hinweg mit der Ausbildung Néelscher Zipfelmützen.

•The spikes, predicted by Néel, were first observed by H.J. Williams* in single crystal silicon-iron [on electrolitically polished (100) surface]:

*H.J. Williams, Phys.Rev. **71**, 646 (1947)

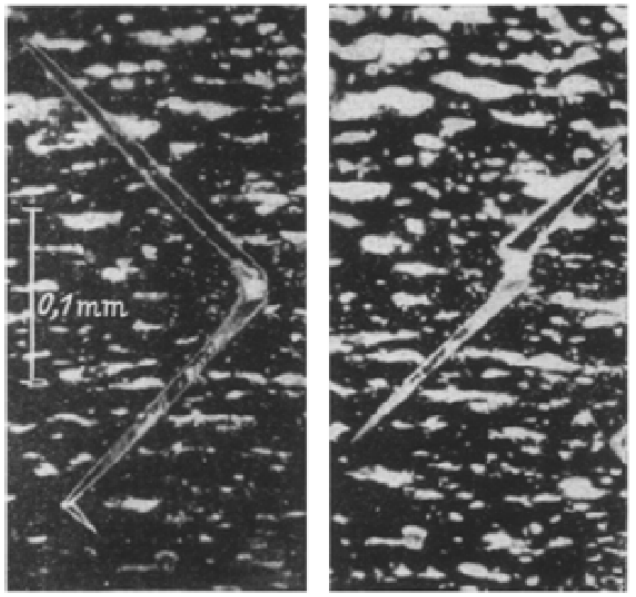

Fig. 13. Zipfelmützenförmige Elementarbereichbildung um kleine Einschlüsse. H. J. Williams.

both images from H. König, Naturwissenschaften **41**, 341 (1954)

Hindrances to domain wall motion

- Grain oriented electrical steel sheet: {110}<001> or {100}<001> crystallographic texture
- Highly anisotropic with one or two magnetic easy axes lying in the sheet plane since the easy axes in Fe–Si lie along the <100> directions.

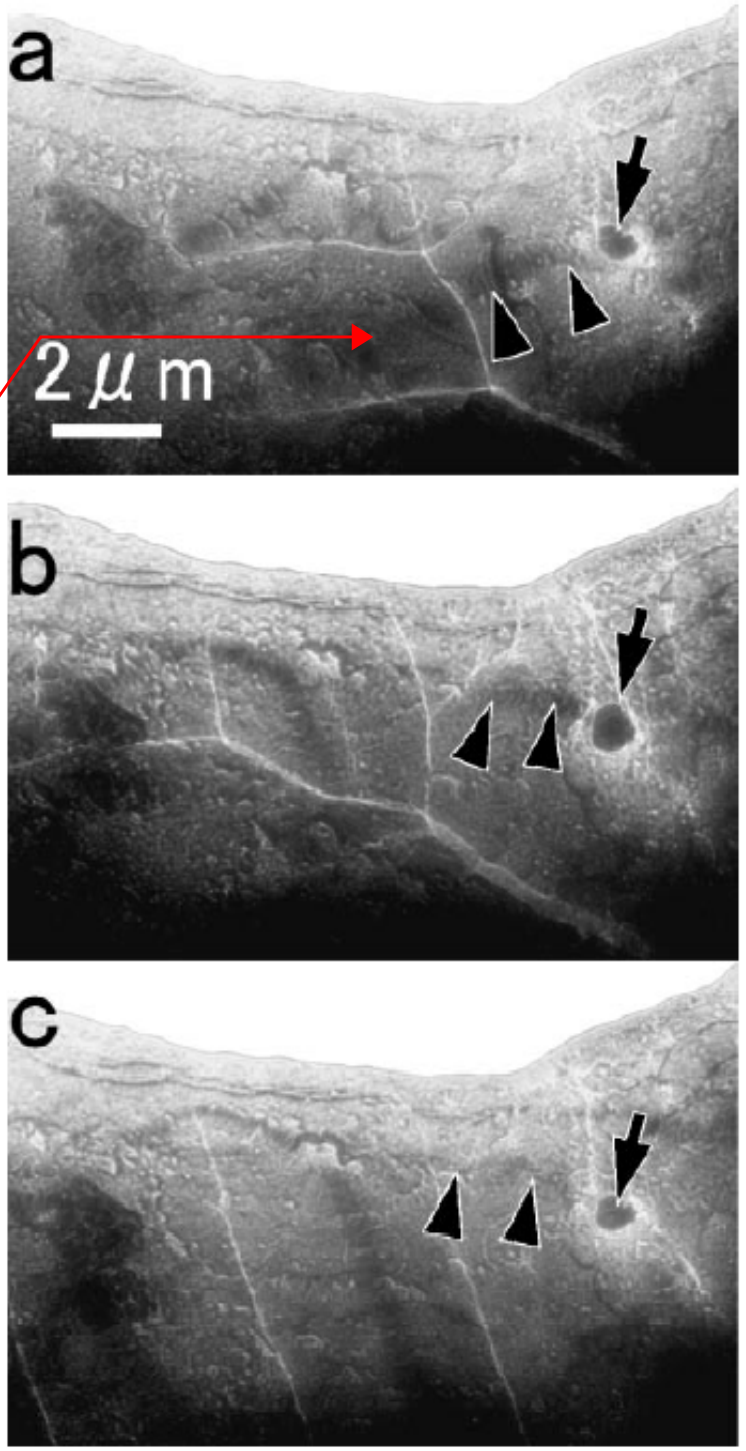

Fig. 4 Lorentz microscope images of a **non-oriented** electrical steel sheet with external magnetic field. The arrow indicates a precipitate in the specimen, and the arrowheads indicate a domain wall which seems to be **pinned at the precipitate**.

Zentaro Akase et al., Materials Transactions **46**, 974 (2005)

Hindrances to domain wall motion - stress

•Residual stress (the stress existing in a body after all external forces have been removed [5]) influences magnetization reversal through stress anisotropy (magnetostriction).
•The stress can be caused by various kinds of crystal imperfections.
•When ferromagnetic material is cooled down below Curie temperature the spontaneous magnetization within each domain distorts the lattice within the domain. As the domains are not free to expand independently the stress field is set up [5].

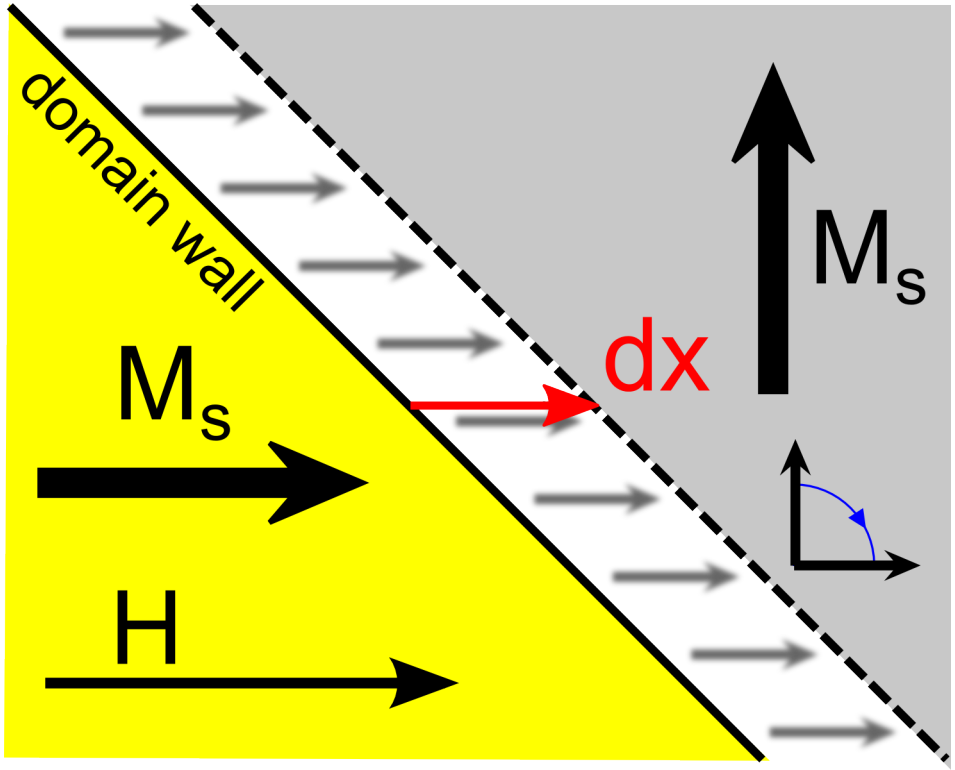

•90° domain wall sweeps from left to right under the influence of external field ***H***
•The movement of the wall effectively corresponds to the reversal of magnetic moments within the area swept by the wall
•Due to stress the energy depends on the orientation of magnetic moments. Let the stress be directed along y-axis*. Then the magnetoelastic energy is given by (see lecture 5):

$$E = -\frac{3}{2}\lambda_{100}\sigma\cos^2\theta$$

•For positive magnetostriction it follows that the stress favors the magnetization along *y* direction.

*it is assumed that the magnetocrystalline anisotropy predominates stress anisotropy so that magnetization in the left domain can be assumed to be parallel to *x*-axis.

Hindrances to domain wall motion - stress

•When the wall moves a distance *d*x the energy of the system changes by [5]*:

$$dE = \frac{3}{2}\lambda_{100}\sigma\, dx - \mu_0 M_s H\, dx$$

it is the energy per unit area of the wall (neglecting cos(45°) factor)

•The stress often depends on the position. Assuming **σ=gx** (σ>0 – tensile stress) we get:

$$dE = \frac{3}{2}\lambda_{100} g\, x\, dx - \mu_0 M_s H\, dx$$

•From equilibrium condition (dE/dx=0) we have as the equilibrium position of domain wall:

$$x = \frac{2}{3}\frac{\mu_0 M_s}{\lambda_{100} g} H$$

It is not generally true that equilibrium position of 90° wall in zero external field corresponds to zero stress [5].

•In case of 180° walls in stressed sample the magnetoelastic energy does not depend directly on the position of the wall as the magnetostrictive strain does not depend on the sense of the magnetization [1].

•The stress influences the domain wall energy of 180° walls so in the stress field it introduces position dependence of energy.

*dependence of 90° wall energy on stress is neglected.

Hindrances to domain wall motion - stress

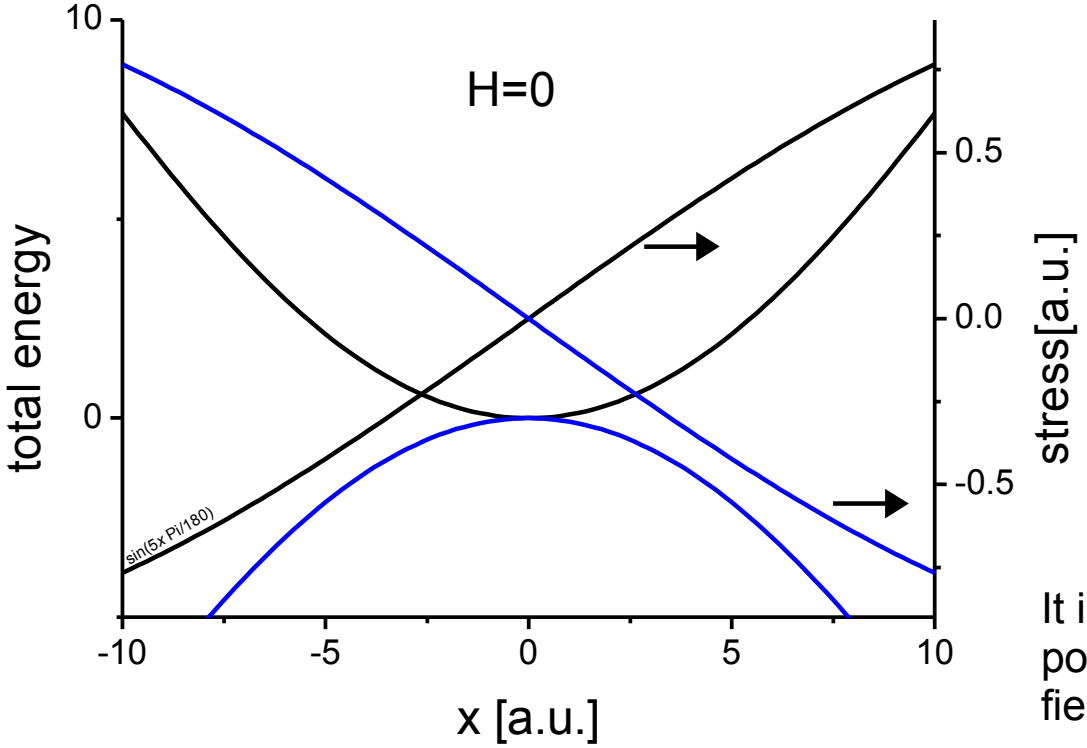

Reversing stress gradient causes the stable wall position (energy minimum) to become **unstable**.

$$E = \frac{3}{2}\lambda_{100}\sigma x$$

It is not generally true that equilibrium position of 90° wall in zero external field corresponds to zero stress [5].

- In case of 180° walls in stressed sample the magnetoelastic energy does not depend directly on the position of the wall as the magnetostrictive strain does not depend on the sense of the magnetization [1].
- The stress influences the domain wall energy of 180° walls so in the stress field it introduces position dependence of energy.

*dependence of 90° wall energy on stress is neglected.

Domain walls and hysteresis

•The reversal of magnetization can involve several processes [6].

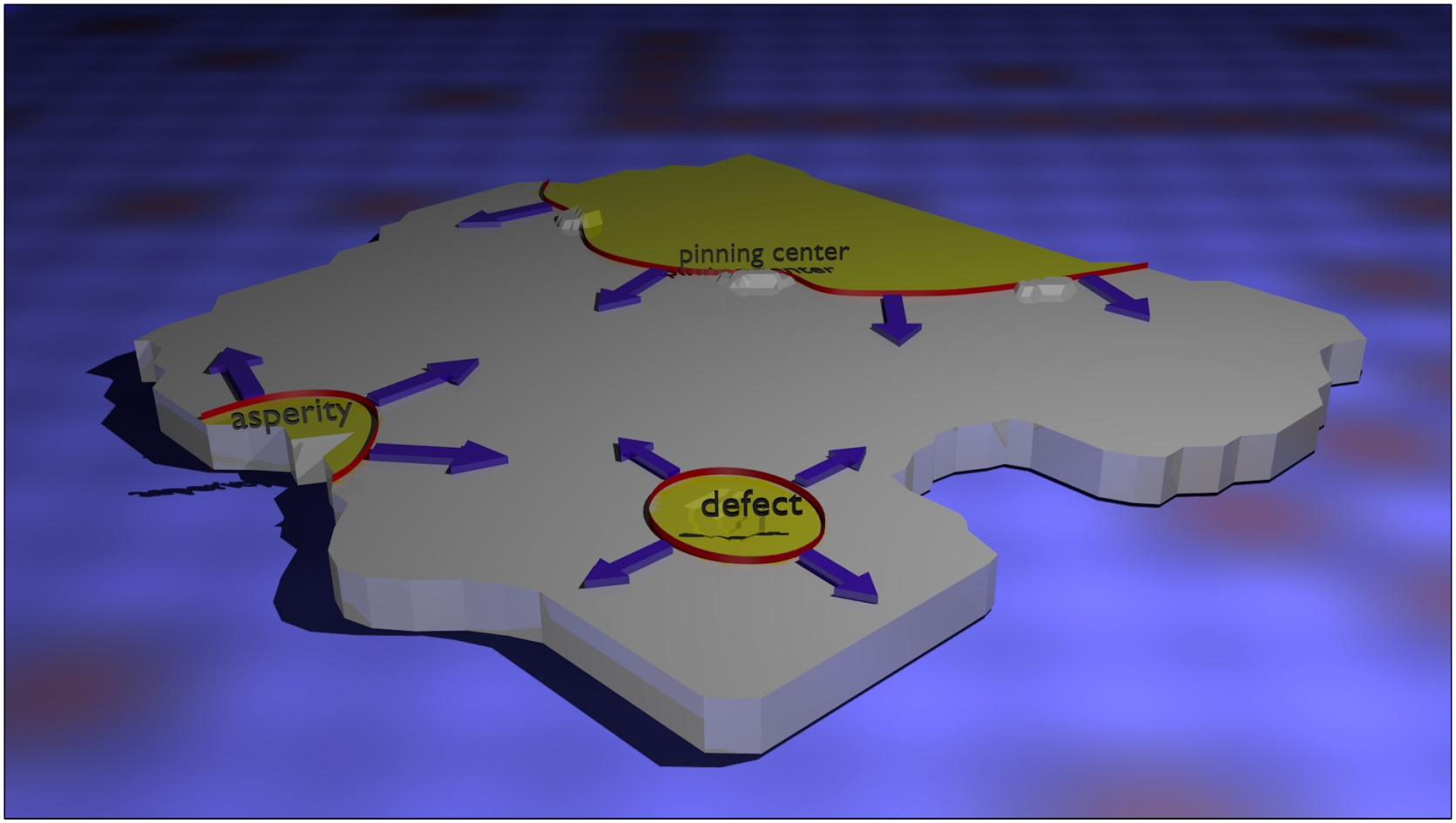

blue arrows show the movement direction of domain wall (red)

•The wall can nucleate at defect, thermal fluctuation, surface asperity
•The movement of wall can be hindered by pinning centers

*graphics based on Fig.7.9 from [6]: J.M.D. Coey, Magnetism and Magnetic Materials, Cambridge University Press 2009

Stripe domains

•In thin films with perpendicular magnetic anisotropy it is possible to observe stripe magnetic domains (see p. 4) magnetized perpendicular to the surface of the film:

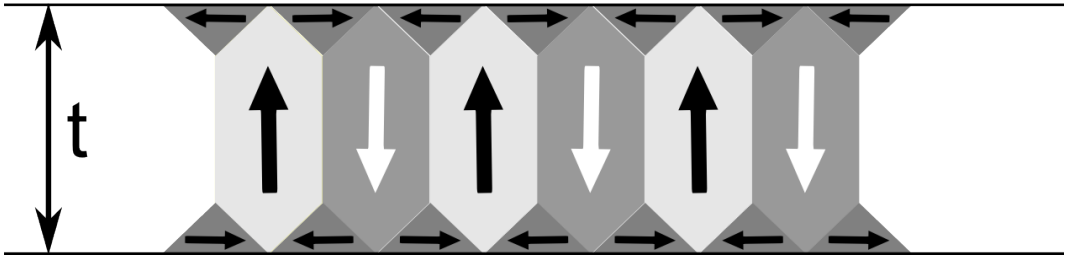

•If perpendicular anisotropy is weak closure domains are observed

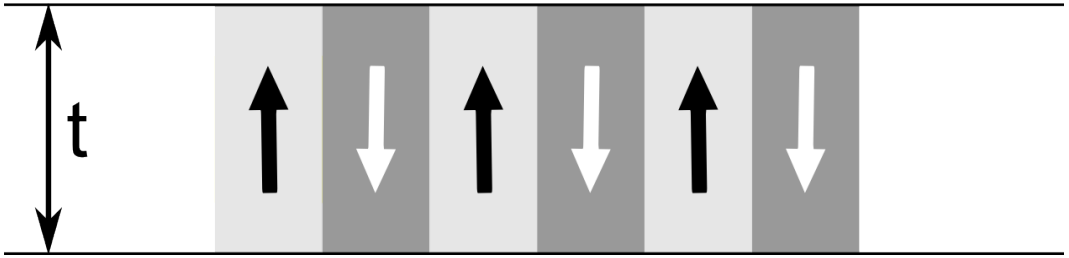

•If perpendicular anisotropy is high closure domains cost to much anisotropy energy and the stripe structure is observed

Stripe domains

•Stripe domains in Co/Au multilayer (MFM images):

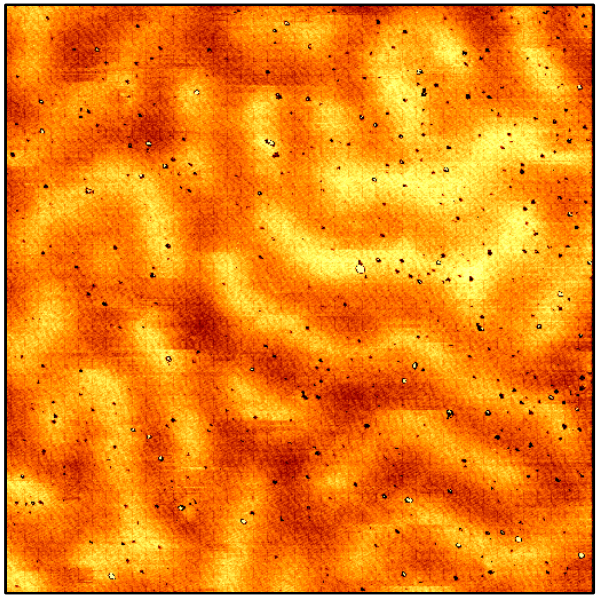

t_{Au}=1.5nm

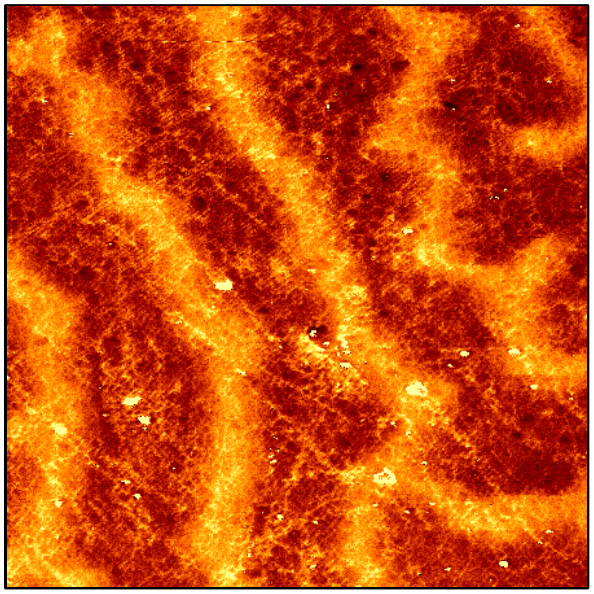

t_{Au}=3nm

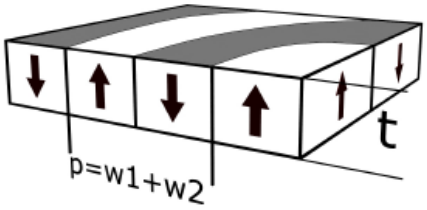

Stripe domains in Si(100)/[$Ni_{80}Fe_{20}$(2 nm)/Au(t_{Au})/Co(1.0nm)/Au(t_{Au})]$_{10}$

Stripe domains

•Period *p* of the stripe domain structure depends on the thickness of the layer [3]:

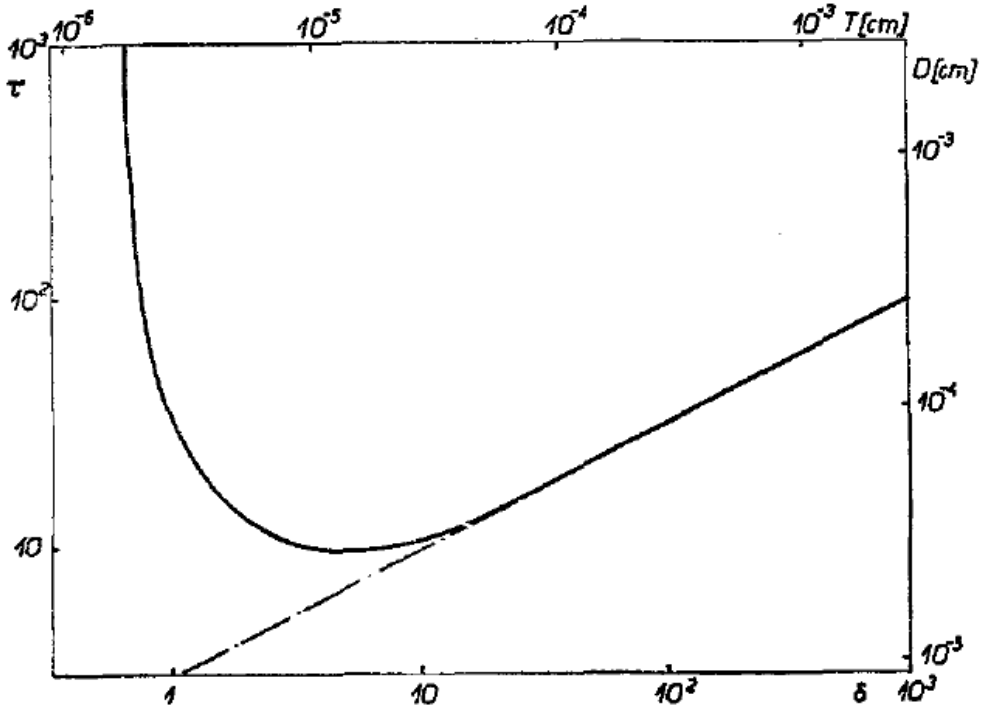

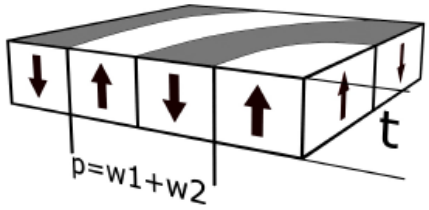

Fig. 2. The width of the domain as a function of the thickness of the film: *a*) general, in the non-dimensional quantities τ and δ (coordinates bottom and left), *b*) for MnBi (coordinates T, D top and right).

For very small thicknesses of the magnetic layers stripe domain period can be in macroscopic range

Z. Málek, V. Kamberský, Czech. J. Phys. **8**, 416 (1958)

Bibliography:

[1] S. Chikazumi, Physics of Magnetism, John Wiley & Sons, Inc., 1964
[2] A. Aharoni, Introduction to the Theory of Ferromagnetism, Clarendon Press, Oxford 1996
[3] A. Hubert, R. Schäfer, Magnetic domains: the analysis of magnetic microstructures, Springer 1998
[4] H. Kronmüller, M. Fähnle, Micromagnetism and the Microstructure of Ferromagnetic Solids, Cambridge University Press, 2003
[5] B. D. Cullity, Introduction to magnetic materials, Addison-Wesley, Reading, Massachusetts 1972
[6] J.M.D. Coey, Magnetism and Magnetic Materials, Cambridge University Press 2009